MEKELLE UNIVERSITY

ETHIOPIA INSTITUTE OF TECHNOLOGY - MEKELLE (EIT-M)

SCHOOL OF MECHANICAL AND INDUSTRIAL ENGINEERING

TRANSPORTATION AND GROUND VEHICLE ENGINEERING

MODELING, SIMULATION, AND FUZZY LOGIC BASED DESIGN AND PERFORMANCE EVALUATION OF A REGENERATIVE BRAKING SYSTEM FOR A CONVERTED 1987 TOYOTA COROLLA ELECTRIC VEHICLE USING MATLAB/SIMULINK

Thesis

Submitted in partial fulfillment of the requirements for the degree of

Masters of Science in Automotive Engineering

By

ADEM MEHAMED YAHYA

Under the supervision of

Dr. Abrha Gebregergs (Associate professor)

Feb 2026

ACKNOWLEDGEMENTS

First and foremost, I want to thank Allah subhanehu wetalla for giving me the strength, patience, and perseverance to complete this work. Without His grace, I would not have reached this milestone.

I am grateful to my thesis supervisor DR. Abraha Gebregergs for their oversight throughout this project. And also want to express my deepest gratitude to my family and friends, who have been my rock during this journey. We have faced so much together due to the instability in our region, yet your unwavering support and love provided the safe harbor I needed to focus and finish this paper. Thank you for believing in me even when the world around us felt uncertain; I truly could not have done this without you.

ABSTRACT

The increasing adoption of electric vehicles has intensified the need for efficiency improvements, particularly in converted electric vehicles constrained by limited battery capacity. Although regenerative braking (RB) is a well-established energy recovery technique, its integration in small-scale vehicle conversions remains limited, and existing implementations often lack optimized control strategies, realistic drive-cycle validation, and comprehensive system-level modeling, leaving critical performance gaps unresolved. This study addresses these challenges through the simulation-based modeling, design, and analysis of a regenerative braking system for a converted 1987 Toyota Corolla electric vehicle, evaluated under the FTP-75 driving cycle. A detailed vehicle and powertrain model was developed in MATLAB/Simulink, incorporating the battery system, electric motor, drivetrain, and a fuzzy logic–based control algorithm designed to dynamically regulate regenerative braking torque under varying operating conditions. The system was evaluated under two scenarios with and without regenerative braking while maintaining an initial battery state of charge (SOC) of 70% to ensure safe charging limits. Simulation results demonstrate that the proposed control strategy effectively enhances energy recovery during frequent stop-and-go urban conditions, increasing the final SOC from 61.79% without RB to 63.04% with RB. This improvement corresponds to a 18% increase in energy efficiency and an extension of driving range by 39.5 km. These results indicate that a properly designed and controlled regenerative braking system can improve energy utilization and driving range in converted electric vehicles, highlighting the potential of fuzzy logic–based control for managing nonlinear braking dynamics.

KEY WORD: *Regenerative Braking; State of Charge (SOC); FTP-75 Drive Cycle; Fuzzy Logic Control; MATLAB/Simulink Modeling; Energy Efficiency; Driving Range Enhancement.*

DECLARATION

Candidate's Declaration

I affirm that this thesis is based on my independent research, except where I have clearly stated otherwise. I have adhered to all the principles of academic honesty and integrity, ensuring that I have not misinterpreted, fabricated, or falsified any information, data, facts, or sources in my work. I understand that violating these principles can lead to disciplinary actions by the Institute and other parties if I have not properly credited them or obtained the necessary permissions.

Name of candidate: Adem Mehamed yahya Signature: _____ Date: 07/04/2026

Advisor's Declaration

This is to certify that the above declaration made by the candidate is correct to the best of my knowledge and the thesis is adequate for the award of the degree of Master of Engineering in Automotive Engineering.

Name of Advisor: Dr. Abrha Gebregergs Signature: _____ Date: 15/04/2026

THESIS ACCEPTANCE APPROVAL FORM

This is to certify that Mr. Adem Mehamed yahya has incorporated all comments forwarded by the external and internal examiners with the chairperson during the thesis defense.

Members of the examination board

Dr. Abrha Gebregergs Supervisor	Signature	15/04/2026 Date
Dr. Getachew Alemayehu External examiner	Signature	08/04/2026 Date
Dr. Asmelash Assefa Internal examiner	Signature	10/04/2026 Date
Tadesse Getaw (MSc) Chairperson	Signature	04/05/26 Date

Confirmation

Head of the Postgraduate and Research Office

Fana Filli Name	Signature	April 27, 2026 Date

Faculty of Mechanical and Industrial Engineering (FoMIE)

Name	Signature	Date

ሚኪኤለ ገ/ኢየሱስ (ዶ/ር)
የሜካኒካልና ኢንዱስትሪያል
ምህንድስና ፋካሊቲ ሃላፊ
Michael G/yesus (PhD)
Head Faculty of Mechanical &
Industrial Engineering

የኢትዮጵያ ቴክኖሎጂ ኢንስቲትዩት-መቐሌ
የሜካኒካልና ኢንዱስትሪያል ምህንድስና ፋካሊቲ
Ethiopian Institute of Technology-Mekelle
Faculty of Mechanical & Industrial Engineering

Abbreviation

BEV	battery electric vehicle
EV	electric vehicle
ICE	internal combustion engine
RB	regenerative braking
RBS	regenerative braking system
SOC	state of charge
BMS	battery management system
PI	proportional–integral
FTP-75	federal test procedure 75 drive cycle
MATLAB	matrix laboratory
PMSM	permanent magnet synchronous motor
DC	direct current
AC	alternating current
KW	kilowatt
N·M	newton-meter
KM	kilometer
S	frontal area of the electric vehicle
ρ	air density
C_d	coefficient of aerodynamic drag

LIST OF TABLES

Table 4. 1: presents the assumed vehicle parameters used throughout the analysis 41
Table 4. 2: Kinetic energy of the vehicle at different velocities 49
Table 4. 3: Relationship between deceleration and braking force 51
Table 4. 4: Stopping Distance at Different Speeds and Deceleration Levels 52
Table 4. 5: power output shaft and battery 55
Table 4. 6: Regenerative Torque and Power Limits at Different Motor Speeds 57
Table 4. 7: Regenerative Deceleration for Different Regenerative Torques 60
Table 4. 8: mechanical power of shaft and electrical power delivered to the battery at different speed at 40N 64
Table 4. 9: kinetic and regenerative force at various speed at 2 m/s² deceleration 74
Table 4. 10: kinetic and regenerative force at various speed at 3 m/s² deceleration 75
Table 4. 11: kinetic and regenerative force at various speed at 6 m/s² deceleration 76
Table 4. 12: battery charging energy limitation during instant regenerative braking 77

Table 5. 1: Result Summary 99

LIST OF FIGURES

figure 2. 1: parallel regenerative braking 14

Figure 3. 1: Fuzzy logic control 32
Figure 3. 2: vehicle body 34
Figure 3. 3: motor block 35
Figure 3. 4: fuzzy logic block 35
Figure 3. 5: battery 36
Figure 3. 6: Mosfet and pulse generator 37
Figure 3. 7: Regenerative braking simulation model in matlab 38
Figure 3. 8: FTP drive cycle 39

Figure 4. 1: Toyota corolla 1987 41
Figure 4. 2: Regenerative Braking Torque Vs Motor speed 58
Figure 4. 3: torque Vs deceleration (regenerative braking) 61
Figure 4. 4: Mamdani-type fuzzy inference system architecture for regenerative braking control, showing input variables and output command 86
Figure 4. 5: Membership functions of brake pedal demand used as a fuzzy input to represent driver braking intention 87
Figure 4. 6: Membership functions of battery state-of-charge (SOC) employed as a fuzzy input to regulate regenerative braking intensity 88
Figure 4. 7: Membership functions of vehicle speed used as a fuzzy input variable in the regenerative braking controller 88
Figure 4. 8: Fuzzy rule base consisting of 27 control rules defining the relationship between inputs to determine the regenerative braking output 90

Figure 5. 1 tunning performance comparison between PID and Fuzzy logic control 93
Figure 5. 2: highlighting energy recovery during stop-and-go events 95
Figure 5. 3: Real-time battery SOC shown in Simulink during without regenerative braking operation 96
Figure 5. 4: Simulink display of battery SOC under FTP-75 drive cycle 97
Figure 5. 5: Real-time battery SOC shown in Simulink during regenerative braking operation 98
Figure 5. 6: Real-time battery SOC shown in Simulink during regenerative braking operation 98

Contents

ACKNOWLEDGEMENTS 2
ABSTRACT 3
DECLARATION ..... **Error! Bookmark not defined.**
LIST OF TABLES .....
LIST OF FIGURES i
CHAPTER ONE 1
1. INTRODUCTION 1
1.1 Background 1
1.2 Problem Statement 2
1.3 Objectives of the Study 2
1.3.1 General Objective 3
1.3.2 Specific Objectives 3
1.4 Scope and Limitations 3
1.5 Significance of the Study 4
1.6 Organization of the Thesis 4
Chapter two 7
2. Literature review 7
2.1 Overview 7
2.2 Introduction to Regenerative Braking 7
2.3 Energy Conversion & Recovery Mechanism 8
2.4 Energy Efficiency Improvements 9
2.5 Influence on Vehicle Dynamics 10
2.6 Weight of converted vehicle 11
2.7 Safety and Stability Considerations 11
2.8 Environmental Benefits 12
2.9 Technicals parts 12
2.9.1 Types of regenerative braking 12
2.9.2 Key Components for Regenerative Braking 14
2.10 Braking Intensity and Energy Recovery Potential 24
2.11 Research gap 24

Chapter three 26
3. Research Methodology 26
3.1 Research Approach and Methodological Framework 26
3.2 Selection and Characterization of the Baseline Vehicle 27
3.2.1 Vehicle Selection 27
3.2.2 Vehicle Parameter Extraction 28
3.3 Powertrain Design and Component Sizing 28
3.3.1 Traction Motor Sizing 29
3.3.2 Energy Storage System (ESS) Design 29
3.4 Regenerative Braking Architecture 30
3.5 Control Strategy Development and Comparative Analysis 30
3.5.1 Proportional–Integral–Derivative (PID) Control 32
3.5.2 Fuzzy Logic Control (FLC) 32
3.6 System Modeling and Simulation Environment 33
3.6.1 Subsystem Modeling 33
3.6.2 Simulation Protocols 38
3.7 Validation and Performance Evaluation 39
Chapter Four 40
4. System design and regenerative braking analysis 40
4.1 Vehicle Description and Design Parameters 40
4.1.1 Base Vehicle and Conversion Overview 40
4.1.2 Key Vehicle Parameters 41
4.1.3 Converted Vehicle Mass Determination 42
4.2 Acting Forces During Vehicle Motion 42
4.3 Required Power at the Wheels 44
4.4 Assumptions for Energy Consumption and Driving Range 45
4.4.1 Regulatory Requirements 46
4.4.2 Design Assumptions 46
4.4.3 Assumptions for average power consumption under nominal driving condition 46
4.4.4 Minimum Usable Battery Capacity 47
4.5 Kinetic Energy and Regenerative Braking Potential 47

4.5.1 Kinetic energy available for recovery 48
4.5.2 Recoverable energy considering system efficiency 48
4.5.3 Classification of Deceleration Levels 49
4.5.4 Required braking force 50
4.5.5 Braking Force at Different Deceleration Levels 51
4.5.6 Stopping Distance at Different Deceleration Levels 52
4.6 Motor-Generator Performance Model 53
4.6.1 Motor Torque-power Characteristics 53
4.6.2 Shaft Power Calculation 54
4.6.3 Regenerative Power Delivered to the Battery 54
4.6.4 Maximum Regenerative Torque Capability 55
4.7 Regenerative Braking Torque and Wheel braking Force 58
4.7.1 Motor Torque to Wheel Torque conversion 58
4.7.2 Regenerative Braking Force at the Wheels 59
4.7.3 Vehicle Deceleration Due to Regenerative Braking 59
4.7.4 Tire–Road Friction Limitation on Regenerative Braking 61
4.7.5 Electrical power generated 62
4.8 Battery and Energy Storage Capacity Verification 65
4.8.1 Energy Recovered During a Single Braking Event 65
4.8.2 Battery Capacity Adequacy Check 66
4.8.3 Maximum Charge Power 66
4.8.4 State of Charge (SOC) Limitation regenerative braking 67
4.9 Brake Force Distribution 68
4.9.1 Brake Force Distribution Strategy 68
4.9.2 Regenerative and Mechanical Braking Allocation 69
4.9.3 Total Required Braking Force and regenerative braking energy 69
4.9.4 Battery-Limited Regenerative braking Power 71
4.9.5 Static Brake Force Distribution 72
4.9.6 Mechanical Braking Requirement 72
4.9.7 Energy recovered and system efficiency for this stop 73
4.10 Instantaneous Regenerative Power Limited by Vehicle Dynamics and Battery Constraints 77

4.11 Thermal Analysis 78
4.11.1 Power loss calculation 78
4.12 Controller calculation 79
CHAPTER 5 93
5. RESULT AND DISCUSSION 93
5.1 Regenerative Braking Functional Validation Using Torque Step Input 93
5.2 FTP-75 Drive Cycle Results with and Without Regenerative Braking 95
Chapter six 102
6. Conclusion 102
Future work 103
Reference 104

CHAPTER ONE

1. INTRODUCTION

1.1 Background

The global transportation sector is one of the significant contributors to the global energy consumption and emission of greenhouse gases. Therefore, electric vehicles (EVs) have gained considerable attention as an environmentally friendly option to conventional internal combustion-based vehicles. Apart from the manufacturing of electric vehicles, the option to convert internal combustion-based vehicles to electric vehicle drives has also gained significant attention due to the cost-effectiveness and suitability for small vehicles. However, the performance and efficiency of electric vehicles obtained through such vehicle conversion methods have limitations.

One of the significant technologies that improve the efficiency of electric vehicle drives is the use of regenerative braking systems. Regenerative braking systems can recover the vehicle's kinetic energy during deceleration and can convert the electric motor to a generator to obtain the electrical energy. which is then stored in the battery. This process reduces overall energy losses, extends driving range, and decreases mechanical brake wear.

In the case of smaller converted vehicles, these challenges become more pronounced. The low mass of the vehicle, the capacity of the batteries, and the control systems need to be well coordinated to provide the regenerative braking torque as well as the conventional friction braking torque to meet the requirements of various driving conditions. If the regenerative braking system has not been designed properly, it can result in inadequate braking, excessive charging of the batteries. Therefore, a systematic design approach is required to balance energy recovery and braking performance while respecting system constraints.

This thesis proposes a simulation-based approach to the design of a regenerative braking system for a converted small vehicle. A detailed vehicle model has been developed to account for the longitudinal motion, electric drive train, battery system, and braking system of the vehicle. The regenerative braking system has been designed to meet the braking force requirements, as well as

the protection of the battery system. The performance of the proposed regenerative braking system has been evaluated using simulation analysis.

This thesis proposes a simulation-based approach to the design of a regenerative braking system for a converted small vehicle. A detailed vehicle model has been developed to account for the longitudinal motion, electric drive train, battery system, and braking system of the vehicle. The regenerative braking system has been designed to meet the braking force requirements, as well as the protection of the battery system. The performance of the proposed regenerative braking system has been evaluated using simulation analysis.

1.2 Problem Statement

Modern electric vehicles are commonly equipped with regenerative braking systems that recover kinetic energy during deceleration, thereby improving energy efficiency, extending driving range, and reducing wear on mechanical braking components. However, small electric vehicles converted from internal combustion engine platforms typically lack integrated regenerative braking systems. As a result, these vehicles rely solely on mechanical braking, leading to significant loss of recoverable energy in the form of heat and reduced overall system efficiency.

Despite the potential benefits, the implementation of regenerative braking in converted electric vehicles presents several challenges. These include the absence of optimized control strategies for torque distribution between regenerative and friction braking, limitations imposed by battery charging constraints and state of charge (SOC), and the nonlinear behavior of the motor and vehicle dynamics under varying driving conditions. Furthermore, existing studies often lack comprehensive simulation-based models that integrate vehicle dynamics, powertrain components, and control systems under realistic driving cycles.

Therefore, there is a need to develop a regenerative braking system tailored for converted small electric vehicles that can intelligently manage braking torque distribution while considering system constraints such as battery limits, motor characteristics, and varying operating conditions. Addressing these challenges is essential to improve energy recovery, enhance driving range, and ensure safe and efficient vehicle operation.

1.3 Objectives of the Study

1.3.1 General Objective

The general objective of this thesis is to design, model, and evaluate a regenerative braking system for a converted 1987 Toyota Corolla electric vehicle using a simulation-based approach in MATLAB/Simulink, with the aim of improving energy recovery, battery state of charge (SOC), and overall vehicle efficiency under standard driving conditions.

1.3.2 Specific Objectives

The specific objectives of this study are to:

- ✓ Calculate the required braking force for the converted small vehicle based on vehicle mass, speed, and deceleration requirements.
- ✓ Estimate the maximum regenerative braking power and potential energy recovery during Deceleration.
- ✓ Develop a simulation model of the vehicle longitudinal dynamics and electric drive train to implement the regenerative braking strategy.
- ✓ Analyze the effect of regenerative braking on battery state of charge (SOC) during the FTP-75 driving cycle.
- ✓ Calculate the improvement in driving range resulting from the application of regenerative braking.
- ✓ Evaluate the energy efficiency of the vehicle by comparing regenerative and non-regenerative braking scenarios.

1.4 Scope and Limitations

This paper has a specific scope, which entails the simulation-based design and evaluation of a regenerative braking system in a converted small electric vehicle. The scope of the project entails

the analytical computation of the braking force, motor torque, regenerative braking power, and charging currents based on the vehicle dynamics.

A longitudinal vehicle dynamics model has been formulated to represent the motion of the vehicle in a straight line. The regenerative braking strategy has been implemented and evaluated using a simulation environment, which comprises the electric motor, power electronics, and the battery system. The regenerative braking system has been evaluated using a representative driving cycle to assess the performance of the regenerative braking system in terms of vehicle speed, state of charge, and regenerative braking impact on driving range. However, the results of this study are limited to simulation results and lack experimental validation on a physical vehicle or test bench. Therefore, the results are valid to the extent of the vehicle, motor, and battery model parameters assumed in the study.

The vehicle dynamics model is limited to longitudinal motion and does not consider vehicle dynamics in the transverse direction, road grade variations, and tire slip effects. Moreover, the thermal effects in the motor, power electronics, and battery are not considered in the model The regenerative braking control strategy is derived on the basis of constant vehicle parameters and does not consider the effects of component aging, battery state of health, and adaptive control in uncertain situations.

1.5 Significance of the Study

This study introduces a structured simulation-based approach for designing and evaluating regenerative braking systems for conversion projects involving small electric vehicles. By addressing the relationship between braking force demands and various electrical constraints such as motor torque and battery charger current capacity, this research contributes to the broader knowledge base regarding the implementation of regenerative braking systems within vehicle conversion projects. The simulation models and methodological approach introduced in this study can be used as a reference for engineers, researchers, and students involved in the conversion of small electric vehicles. The results obtained in this research can also be used for informed decision-making during the early stages of designing regenerative braking systems for

small electric vehicles. Moreover, the results obtained in this study also show the potential influence of regenerative braking systems on the state of charge of batteries as well as the driving range of small electric vehicles. The approach introduced in this study can be used for designing regenerative braking systems for conversion projects involving small electric vehicles.

1.6 Organization of the Thesis

This thesis has a total of six chapters, which have been designed to systematically address the analysis, design, modeling, simulation, and evaluation of a regenerative braking system of a converted small electric vehicle.

Chapter 1: Introduction

This chapter outlines the background of the research, which mainly focuses on the importance of regenerative braking in the enhancement of the efficiency of converted electric vehicles. The problem statement, objectives, scope, significance, and questions of the research have been well defined. The outline of the thesis has been given.

Chapter 2: Literature Review

This chapter discusses the literature review of the existing literature on the conversion of electric vehicles, conventional braking systems, regenerative braking systems, and control strategies of regenerative braking systems. The modeling techniques, regenerative braking, and performance evaluation have been critically discussed to identify the gap in the literature, which has led to the motivation of the research work.

Chapter 3: System Modeling and Research Methodology

This chapter discusses the overall research methodology and system modeling approach. In this regard, the mathematical models of the vehicle longitudinal dynamics, electric motor, power electronics, battery system, and braking forces will be discussed. The simulation environment,

assumptions, control strategy, and performance indicators will be explained in this chapter as well.

Chapter 4: Regenerative Braking System Design and Control Development

In this chapter, the design of the proposed regenerative braking system will be introduced from an engineering perspective. In other words, the design objectives and constraints such as safety considerations in braking, tracking of driver demand, battery charging limits, and motor torque limits are identified. With these constraints in mind, the regenerative braking system will be designed and developed, including torque allocation, blending of regenerative and mechanical braking, and selection of various control parameters. In addition, the rationale of each of these design decisions will be addressed and implemented within the simulation framework.

Chapter 5: Results and Discussion

In this chapter, the results obtained from the simulation using the standard driving cycles and braking conditions will be presented and analyzed. The performance of the proposed regenerative braking system will be critically evaluated based on the obtained results, and the results will be compared with the relevant results obtained from the existing literature.

Chapter 6: Conclusion and Future Work

In this final chapter of the thesis, the overall results and the contributions of the work will be highlighted. The conclusions of the work will be drawn based on the results obtained from the work. The limitations of the work will be acknowledged, and the recommendations for the future work will be proposed.

CHAPTER TWO

2. LITERATURE REVIEW

2.1 Overview

The role of the literature review is vital in the understanding of the current status of the research and technological advancements regarding the regenerative braking systems for electric vehicles. This section lays the groundwork for the current research by identifying the various theories, principles, and methodologies that have already been explored by various researchers. This section offers an insight into the various advancements, challenges, and gaps that the current research is intended to address.

The simulation-based design of regenerative braking for converted small electric vehicles has become an area of significant interest due to the potential for energy efficiency, driving range, and braking performance improvements. The emphasis on sustainable transport solutions has also increased the need for the integration of regenerative braking systems for converted electric vehicles, as this is seen as an effective way of saving energy without the need for complete vehicle redesigns. This is an area of research that involves the principles of electric motor control, power electronics, and vehicle dynamics for the optimization of regenerative braking energy recovery systems.

This literature review will follow a pattern that creates a comprehensive foundation for the simulation-based design of a regenerative braking system of a converted small EV. It will start by presenting the theoretical foundations of regenerative braking systems, including their energy conversion principles and efficiency and dynamics implications on vehicle safety and environmental impact. It will then focus on the different regenerative braking system types, such as series and parallel types of regenerative braking systems, supported by various studies carried out by different researchers. It will also focus on different regenerative braking system components such as battery types, electric motors, and power electronic interfaces and their implications on regenerative braking system design.

Additionally, it will focus on different regenerative braking system controls such as PID, fuzzy logic, and intelligent model based controls and their implications and limitations. It will then focus on research gaps concerning regenerative braking systems, particularly in relation to simulation based designs of converted small EVs and their implications and limitations in the Ethiopian context.

2.2 Introduction to Regenerative Braking

Regenerative braking in electric vehicles (EVs) refers to the process of converting the vehicle's kinetic energy during deceleration into electrical energy, which is subsequently stored in the energy storage system. This is achieved by operating the traction motor in generator mode, allowing mechanical energy from the drivetrain to be converted into electrical energy and redirected to the battery or auxiliary storage devices such as super capacitors (Totev et al., 2019; Shanmugapriya et al., 2024).

From a system perspective, regenerative braking is not only an energy recovery mechanism but also a controlled electromechanical process involving motor control, power electronics, and energy storage coordination. Studies have implemented control strategies such as Direct Torque Control (DTC) and fuzzy logic to regulate braking torque distribution between regenerative and friction braking systems (Gulhane et al., 2024). These approaches aim to maximize energy recovery while maintaining vehicle stability and braking performance.

Despite its advantages, regenerative braking is inherently limited by system constraints, including motor capacity, battery charging limits, and vehicle operating conditions. Under high braking demand or fully charged battery states, the system cannot recover all available energy, resulting in reliance on mechanical braking and associated energy losses (Shanmugapriya et al., 2024). These limitations highlight the need for optimized control and system-level modeling in regenerative braking design.

2.3 Energy Conversion & Recovery Mechanism

The regenerative braking process is governed by the principle of energy conservation, where the vehicle's kinetic energy is partially converted into electrical energy during deceleration. This is achieved by applying negative torque through the electric motor, causing it to function as a generator via electromagnetic induction (Fam, 2022; Vasiljević et al., 2022).

From a modeling and simulation standpoint, the process can be represented through three interacting subsystems:

- Energy conversion: mechanical-to-electrical conversion via the motor-generator
- Energy storage: transfer and storage of electrical energy in the battery through power electronic converters
- Control system: regulation of torque and power flow based on operating conditions

Previous studies have implemented these subsystems using simulation environments to evaluate regenerative braking performance. For instance, Ahmad (2024) and Doss et al. (2023) modeled motor energy conversion characteristics, while Kale et al. (2023) focused on power electronic interfaces for efficient energy transfer. Control strategies such as fuzzy logic have been applied to dynamically regulate regenerative torque based on parameters such as vehicle speed and battery state of charge (Gulhane et al., 2024).

The total recoverable energy is fundamentally constrained by the vehicle's kinetic energy, expressed as:

$$E_K = {}^1\!/_2\ mv^2$$

where m is the vehicle mass and v is its speed.

However, in practical systems, not all kinetic energy can be recovered due to losses associated with aerodynamic drag, rolling resistance, drivetrain inefficiencies, and battery charging limitations. Studies such as Melis and Chishty (2013) emphasize that accurate estimation of recoverable energy requires incorporating these vehicle dynamics and system constraints into simulation models. Therefore, effective regenerative braking design relies on integrating vehicle dynamics, control strategies, and energy storage limitations to optimize energy recovery while ensuring vehicle stability and drivability.

2.4 Energy Efficiency Improvements

Regenerative braking systems significantly enhance the energy efficiency of electric vehicles by Regenerative braking systems contribute significantly to improving the overall energy efficiency

of electric vehicles by recovering energy that would otherwise be dissipated as heat during braking. However, the extent of efficiency improvement depends heavily on the control strategy, system configuration, and driving conditions.

Simulation-based studies have reported energy recovery efficiencies ranging from 8% to 25% under standard driving conditions (Zhe et al., 2017). Additionally, the integration of optimized braking torque control strategies has demonstrated substantial improvements in urban driving cycles, with energy recovery enhancements of up to 37.8% (Faghihian et al., 2024).

Methodologically, these improvements are achieved through:

- torque distribution optimization algorithms
- adaptive control strategies (e.g., fuzzy logic, model-based control)
- enhanced energy storage systems (e.g., hybrid battery–supercapacitor configurations)

Hamdan et al. (2023) utilized capacitor-assisted storage systems to improve transient energy capture during braking events, while Xu et al. (2016) demonstrated that electrically controlled braking systems outperform conventional hydraulic systems in terms of controllability and recovery efficiency.

Despite these advancements, efficiency gains remain highly dependent on real-world operating constraints such as battery state of charge, vehicle speed, and braking intensity. This reinforces the importance of simulation-based approaches for evaluating and optimizing regenerative braking performance under varying conditions.

2.5 Influences on Vehicle Dynamics

Regenerative braking can also contribute to improved driving performance by improving the response and dynamics of the vehicle's braking system. This can be achieved through dual control techniques and sophisticated torque management algorithms that can improve the distribution of braking force, thus improving stopping time and vehicle handling (Gulhane et al., 2024). Moreover, sophisticated adaptive control algorithms such as knowledge-based systems can improve vehicle stability by enabling real-time adaptation of vehicle braking characteristics according to tire-road conditions, thus improving stability without complex calculations (Xu et al., 2016). This can improve not only regenerative braking efficiency but also vehicle handling and drivability, thus improving the vehicle's braking experience (Qian et al., 2018).

2.6 Weight of converted vehicle

An increase in the weight of retrofitted EVs is an essential factor in the transition from ICE vehicles. This is because the retrofitting process involves the addition of components such as batteries and electric motors. This addition of components is bound to increase the total weight of the vehicle. Studies show that the increase in the total weight of retrofitted vehicles is estimated at about 11.5% (Duangtongsuk et al., 2022). The increase in the weight of the vehicle is likely to increase road wear and tear (Low et al., 2022).

2.7 Safety and Stability Considerations

Safety and vehicle stability are major factors to be considered in the design of a regenerative braking system. Sophisticated braking techniques ensure that the optimal amount of torque is delivered to the vehicle to prevent wheel lock and provide vehicle stability in different braking scenarios (Xu et al., 2011). Knowledge-based and adaptive techniques overcome the problems that occur in the vehicle, such as slip calculation, load transfer, and road surface variations, to provide vehicle stability while optimizing regenerative energy capture (Xu et al., 2016). Moreover, specific vehicle control techniques are used in low-speed scenarios to provide vehicle stability, which enhances safety as well as driver confidence (Wang et al., 2024).

2.8 Environmental Benefits

The environmental benefits of regenerative braking can be explained by the fact that regenerative braking helps to reduce the use of friction brakes, which improves the efficiency of the system. Regenerative braking, therefore, improves the efficiency of electric vehicles by reducing the amount of energy consumed by the vehicle, which in turn reduces the particulate matter emitted by the vehicle as a result of the use of friction brakes (Qian et al., 2018). The efficiency of the regenerative braking system, therefore, improves the sustainability of the environment as far as electric vehicles are concerned.

2.9 Technical parts

2.9.1 Types of regenerative braking

a. Series Regenerative Braking

Series regenerative braking is characterized by the coordinated operation of the electric motor and mechanical braking system, where the motor primarily provides braking torque through energy regeneration, while friction brakes supplement the required braking force under higher demand conditions.

From a methodological perspective, studies on series regenerative braking focus on torque distribution strategies that maximize energy recovery while maintaining vehicle stability. Control approaches such as fuzzy logic, neural networks, and predictive algorithms have been implemented to dynamically allocate braking force between regenerative and mechanical systems based on real-time vehicle parameters (Xu et al., 2011; Liu, 2021; Li et al., 2023). These methods are typically evaluated using simulation environments under varying driving conditions and battery states of charge.

Reported results indicate that series regenerative braking systems can achieve energy recovery improvements in the range of 20–25% compared to non-regenerative systems, with performance highly dependent on control strategy and operating conditions (Zhang et al., 2008; Li et al.,

2020). Further enhancements have been demonstrated through the integration of hybrid energy storage systems, which improve transient energy capture and overall system efficiency (Naseri et al., 2017).

In addition to energy performance, system stability and safety remain critical evaluation criteria. Research has incorporated slip control and anti-lock braking constraints within control algorithms to prevent wheel lock and ensure smooth braking under different road conditions (Xu et al., 2011; Xiao et al., 2017). Experimental and simulation-based validations confirm that properly designed series regenerative braking systems can achieve a balance between energy recovery, drivability, and safety, making them a well-established approach for modern EV applications (Barroso et al., 2023; Salari et al., 2023).

b. Parallel Regenerative Braking

Parallel regenerative braking systems improve the energy efficiency of electric vehicles by Parallel regenerative braking systems operate by allowing the electric motor and mechanical braking system to function simultaneously, where regenerative braking is applied up to the motor's capability, and additional braking demand is met by friction brakes. This configuration facilitates easier integration with conventional hydraulic braking systems but may limit maximum energy recovery due to motor constraints (Bian & Qiu, 2017).

Methodologically, research on parallel regenerative braking emphasizes braking force blending strategies, where control algorithms determine the optimal distribution of torque between regenerative and mechanical braking systems. Simulation-based studies have widely applied fuzzy logic and adaptive control techniques to optimize this distribution under varying vehicle speeds and driving conditions (Yuantao et al., 2019).

Advanced implementations, such as the Improved Parallel Regenerative Braking System (IPRBS), have demonstrated measurable performance gains, including reductions in energy consumption and improvements in driving range, while maintaining driver-perceived braking characteristics (Mondal & Nandi, 2022). Additionally, the integration of supercapacitors

alongside batteries has been shown to enhance high-power energy absorption during braking events, reducing battery stress and improving overall system durability (Harshavardhan et al., 2024).

Simulation analyses further indicate that optimized parallel regenerative braking strategies are particularly effective in urban driving cycles, where frequent braking events allow greater energy recovery potential (Jing-ming et al., 2008). However, system performance remains dependent on control precision, motor capacity, and energy storage limitations.

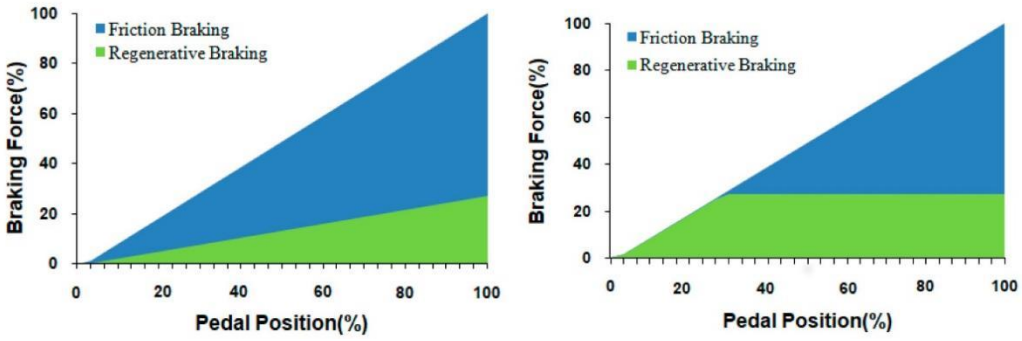

Figure 2. 1: parallel regenerative braking (Shepard, J. (2024)

2.9.2 Key Components for Regenerative Braking

I. Suitable Battery Technologies

The selection of battery technology is a critical design consideration in regenerative braking systems, as it directly affects energy recovery efficiency, charge acceptance rate, and system durability. Unlike conventional EV operation, regenerative braking involves high power, short-duration charge pulses, requiring storage systems with fast charge–discharge capability and high cycle life.

From a methodological perspective, existing studies evaluate battery technologies based on parameters such as:

- specific energy and power density
- charge acceptance rate during regenerative events
- cycle life under frequent charge–discharge conditions
- thermal stability and safety

Lithium-ion batteries, particularly Lithium Iron Phosphate ($LiFePO_4$), are widely adopted in regenerative braking applications due to their high thermal stability, long cycle life, and moderate power capability. Comparative studies indicate that $LiFePO_4$ batteries outperform other lithium-ion chemistries in terms of reliability and lifespan under repeated regenerative cycling conditions. In contrast, Lithium Titanate (LTO) batteries demonstrate superior charge acceptance and extremely long cycle life, making them suitable for high-power regenerative applications, although at the expense of lower energy density.

Lower-cost alternatives such as lead-acid and nickel-cadmium batteries have been evaluated in the literature; however, their limited cycle life, low charge efficiency, and poor high-rate charging capability make them unsuitable for regenerative braking systems, where rapid energy absorption is required (Das et al., n.d.; Bhoopal et al., 2025). Although economically attractive, these technologies introduce performance limitations that negatively impact overall system efficiency and durability.

To address the limitations of standalone battery systems, several studies have proposed hybrid energy storage systems (HESS) combining batteries with super capacitors. In such configurations:

- the battery provides energy capacity
- the super capacitor handles high-power transient energy during braking

Simulation and experimental studies (Alam, 2024; Patle & Subha, 2023) show that this approach:

- improves energy recovery efficiency

- reduces battery stress and degradation
- enhances overall system responsiveness

Environmental and operational conditions also influence battery selection. Factors such as temperature, charging infrastructure, and recycling availability affect long-term sustainability and feasibility, particularly in developing regions. Lithium-ion technologies generally provide lower lifecycle environmental impact when proper recycling systems are available (Brunner & Brunner, 2021).

Overall, the literature indicates that Li-ion batteries (especially $LiFePO_4$), combined with super capacitors in hybrid configurations, offer the most effective solution for regenerative braking systems. However, optimal selection depends on system-level trade-offs between cost, performance, and operating conditions, which must be evaluated through simulation-based design approaches.

II. Suitable Motor Technologies

The selection of an appropriate motor is a critical factor in electric vehicle (EV) conversion, as it directly influences both propulsion performance and regenerative braking capability. In regenerative systems, the motor must operate efficiently in both motoring and generating modes, requiring high torque controllability, fast dynamic response, and efficient energy conversion.

From a methodological perspective, motor technologies are evaluated based on:

- efficiency in motoring and generating modes
- torque–speed characteristics
- regenerative braking capability (negative torque control)
- control complexity and converter requirements
- thermal performance and reliability

Among available technologies, Permanent Magnet Synchronous Motors (PMSM) are widely used due to their high efficiency, high torque density, and superior dynamic response, making

them suitable for both propulsion and regenerative braking applications (Zheng, 2022). Their ability to deliver precise torque control enables effective energy recovery, particularly when integrated with advanced control strategies.

Brushless DC (BLDC) motors are also strong candidates for regenerative braking systems, offering high efficiency, good speed control, and relatively simpler control implementation compared to PMSMs. Studies have shown that BLDC motors can achieve effective regenerative energy recovery across varying speed ranges due to their favorable torque characteristics and responsiveness (Doss et al., 2023; Riyadi & Setianto, 2019; Esfahani et al., 2024). In simulation-based implementations, BLDC motors are often coupled with bidirectional DC–DC converters to enable controlled energy flow during braking and acceleration.

Switched Reluctance Motors (SRMs) present advantages in terms of robustness, fault tolerance, and low manufacturing cost. Their simple construction makes them attractive for harsh operating conditions; however, their torque ripple and control complexity can limit smooth regenerative braking performance. Nevertheless, research indicates that SRMs can achieve competitive acceleration and acceptable regenerative performance when advanced control strategies are applied (Yildirim et al., 2014; Farzana & Bindu, 2022).

Induction Motors (IMs) are valued for their cost-effectiveness, durability, and ease of control, and have been widely used in EV applications. However, compared to PMSM and BLDC motors, IMs generally exhibit lower efficiency and reduced regenerative performance, particularly at low speeds, which can limit energy recovery effectiveness (Yildirim et al., 2014).

From a system integration perspective, motor performance in regenerative braking is strongly influenced by the power electronic interface and control strategy. Advanced converter topologies, such as bidirectional and modular multilevel converters, are employed to regulate power flow and minimize losses during regeneration (Riyadi & Setianto, 2019; Esfahani et al., 2024).

Overall, the literature indicates that PMSM and BLDC motors provide the most suitable balance of efficiency, controllability, and regenerative performance for EV conversion applications. While SRMs and IMs offer advantages in cost and robustness, their limitations in control smoothness and efficiency must be carefully considered. Therefore, motor selection should be based on a system-level evaluation of performance requirements, control strategy, and cost constraints, typically validated through simulation-based design approaches.

III. Control Strategies

Control strategies play a critical role in regenerative braking systems, as they determine the distribution of braking torque**,** energy recovery efficiency**,** and vehicle stability under varying operating conditions. In simulation-based design, control algorithms are typically evaluated based on their ability to regulate negative motor torque**,** respond to dynamic inputs, and operate under system constraints such as battery state of charge (SOC) and vehicle speed.

A. Traditional Proportional-Integral-Derivative (PID) control

Proportional–Integral–Derivative (PID) control is one of the most widely used conventional control strategies in regenerative braking systems due to its simple structure, ease of implementation, and fast response characteristics. In these systems, PID controllers are typically used to regulate motor speed or braking torque by minimizing the error between desired and actual system outputs.

From a methodological standpoint, PID control operates based on:

- error input (difference between reference and actual value)
- proportional, integral, and derivative gains
- real-time feedback loop for torque regulation

In regenerative braking applications, PID controllers are commonly applied to Brushless DC (BLDC) motor control, where they provide stable and predictable torque response during energy recovery (Kelin, 2015). Simulation studies show that PID control is effective under steady and

moderately varying conditions, ensuring consistent braking performance and acceptable energy recovery.

However, a key limitation of PID control is its dependence on accurate tuning and fixed control parameters, which reduces its effectiveness under highly dynamic conditions such as varying road surfaces, changing vehicle speeds, and fluctuating battery SOC. As a result, PID-based systems may not fully optimize energy recovery in complex real-world driving scenarios.

B. Fuzzy Logic Control

Fuzzy logic control (FLC), as a popular method, can be effectively used in regenerative braking Fuzzy Logic Control (FLC) has been widely adopted in regenerative braking systems to address the limitations of conventional controllers by providing adaptive and rule-based decision-making. Unlike PID control, FLC does not rely on precise mathematical models but instead uses linguistic rules and membership functions to handle nonlinear and uncertain system behavior.

Methodologically, FLC operates based on:

- input variables (e.g., vehicle speed, braking demand, battery SOC)
- fuzzy rule base (IF–THEN rules)
- inference mechanism and defuzzification process
- output control signal for torque distribution

In regenerative braking applications, fuzzy logic controllers are used to dynamically allocate braking force between regenerative and friction braking systems. Studies have demonstrated that FLC can effectively adjust pulse-width modulation (PWM) signals in real time to ensure smooth transitions and maximize energy recovery (Karabacak & Uysal, 2020).

Simulation-based analyses indicate that FLC performs well under variable driving conditions, including urban stop-and-go scenarios, where braking demand and system states change rapidly (Aksjonov et al., 2020). Additionally, FLC has been successfully integrated with anti-lock

braking systems (ABS) to improve vehicle stability while maintaining efficient energy recuperation.

Despite its advantages, FLC introduces higher design complexity, including the need for rule definition, membership function tuning, and defuzzification selection. In some cases, its response time may be slower than PID control, depending on system design.

Defuzzification

Defuzzification is a critical stage in fuzzy logic control systems, where the aggregated fuzzy output obtained from the inference mechanism is converted into a crisp control signal suitable for real-time implementation. In regenerative braking applications, this output typically represents the regenerative braking torque or torque distribution ratio.

From a control perspective, the choice of defuzzification method directly influences:

- torque smoothness
- system response time
- stability during braking transitions

Several defuzzification techniques have been applied in regenerative braking control systems:

- Center of Gravity (CoG):
  This method computes the centroid of the aggregated fuzzy set, producing a smooth and continuous output. It is widely used in simulation-based studies due to its ability to provide stable and balanced torque control, making it suitable for maintaining vehicle stability during regenerative braking (Kumar, 2017).
- Mean of Maximum (MoM):
  This approach averages the values corresponding to the maximum membership degree. While computationally simpler, it may result in less smooth control output, which can affect braking comfort and stability in dynamic conditions (Gilda & Satarkar, 2020).

- Improved Semi-Linear Methods:

  Advanced defuzzification techniques have been developed to reduce steady-state error and overshoot, improving control precision in systems with rapidly changing inputs such as vehicle speed and braking demand (Na & Jing, 2012).

In simulation studies of regenerative braking systems, the selection of defuzzification method is typically based on a trade-off between computational complexity and control performance. Methods such as CoG are preferred for applications requiring smooth torque variation, while simpler methods may be used where computational efficiency is prioritized.

However, due to the inherent uncertainty in fuzzy systems, the performance of defuzzification methods may vary under different operating conditions. This highlights the importance of careful method selection and validation through simulation, particularly in applications involving variable driving conditions and battery constraints (Mallick & Das, 2021; Zhijian, 2006).

IV. Power Electronics

Power electronic systems form the backbone of regenerative braking, as they enable controlled energy transfer between the motor, battery, and auxiliary components. In simulation-based regenerative braking design, power electronics are evaluated based on their ability to regulate bidirectional power flow, maintain voltage stability, and operate efficiently under dynamic conditions.

a. DC-DC Converter

DC–DC converters are essential for managing the energy exchange between the electric motor and the battery during both motoring and regenerative braking modes. Their primary function is to ensure voltage matching and controlled power transfer, enabling efficient storage of recovered energy.

From a system perspective, converter performance is assessed based on:

- bidirectional power flow capability

- conversion efficiency
- voltage regulation under dynamic load conditions
- integration with control algorithms

1. **Bidirectional DC-DC Converters**

Bidirectional DC–DC converters are widely used in regenerative braking systems due to their ability to support energy flow in both directions:

- motoring mode: battery → motor
- regenerative mode: motor → battery

These converters typically operate in:

- boost mode during motoring
- buck mode during regenerative braking

Control is commonly implemented using PI-based feedback controllers operating in Continuous Conduction Mode (CCM), ensuring stable voltage regulation and efficient energy transfer (Kannan et al., 2023).

Advanced configurations have been proposed to enhance performance under varying conditions:

- tri-mode converters (buck–boost–buck-boost): improve efficiency at low speeds and varying voltage levels (Dias et al., 2024)
- non-isolated high-gain converters: increase voltage adaptability for different operating conditions (Kumar et al., 2021)

These designs are typically validated through simulation to evaluate efficiency, voltage stability, and response under regenerative events.

2. **Multi-port and SIMO Converters**

Multi-port converters extend system functionality by integrating multiple energy sources**,** such as batteries and supercapacitors, into a unified power management system. This allows simultaneous energy distribution and improves overall system efficiency and flexibility (Irshana & Vijayasree, 2025).

Similarly, Single-Input Multiple-Output (SIMO) converters provide multiple voltage levels for different subsystems, enabling coordinated energy management during both driving and braking conditions (Suresh et al., 2022).

These converter topologies are particularly relevant in hybrid energy storage systems**,** where efficient allocation of regenerative energy is required.

Torque Control and Converter Role

DC-DC converters operate in conjunction with the (BMS) to control the regenerative braking torque and optimize the regenerative braking process. Dynamic torque calculation methods can be used to find the maximum allowable regenerative torque during the braking process (Minarcin et al., 2010). Torque distribution methods can also be used to improve the performance of the vehicle during the braking process by controlling the regenerative and hydraulic braking forces. At the same time, the methods can prevent the wheels from slipping and improve the safety of the vehicle (Tousi et al., 2016). In this context, the bidirectional DC-DC converter plays an important role in controlling the regenerative and motor acceleration process. In the buck mode, the DC-DC converter can supply the required power to the battery during the regenerative process. Similarly, the DC-DC converter can supply the required power to the motor during the acceleration process (Kannan et al., 2023). The voltage matching between the battery and motor is important to improve the efficiency and performance standards during the regenerative process.

b. **Battery Management Systems**

Battery Management Systems (BMS) are a key factor in the regenerative braking system, as they ensure the safe and efficient operation of the system. The BMS is responsible for monitoring the battery status and its charging limits, thus allowing the regenerative braking system to provide the optimal amount of energy to the battery without exceeding the safety limits (Faghihian et al., 2024). The system is responsible for regulating the voltage and current supplied to the battery to prevent excessive charging and discharging, thus increasing the life of the battery.

In addition to the safety features, the BMS is a key factor in the energy management system. During the operation of the regenerative braking system, the BMS regulates the voltage supplied to the battery to the desired limits, thus providing the optimal amount of energy to the battery from the motor (Suresh et al., 2022). The efficient operation of the BMS in the regenerative braking system allows the efficient distribution of energy to the battery, thus providing the optimal amount of energy to the battery. Thus, the efficient operation of the BMS in the regenerative braking system is essential in optimizing the efficiency of the system.

2.10 Braking Intensity and Energy Recovery Potential

The deceleration rate during regenerative braking varies with driving conditions and the control strategies implemented, directly influencing energy recovery and vehicle stability. Braking intensity is generally categorized as gentle, firm, or aggressive.

a. Gentle braking: with an acceleration rate of 0.1-0.3 g (0.98-2.9 m/s²), is applicable for regular stoppages such as stop signs, as it offers moderate energy recuperation while focusing on the comfort of the driver ("Optimal Deceleration Zone of EV with an…," 2023).

b. Firm braking: with an acceleration rate of 0.3-0.5 g (2.9-5.8 m/s²), is applicable for critical stoppages such as emergencies, as it offers maximum energy recuperation potential due to the conversion of considerable amounts of kinetic energy (Melis & Chishty, 2013).

c. Aggressive braking: with an acceleration rate of 1.0 g (6-9.8 m/s²), is applicable for high-speed driving or critical deceleration, as it offers maximum energy recuperation potential while focusing on the comfort of the driver (Sim et al., 2019). This differentiation helps regenerative braking systems achieve the maximum potential for energy recuperation while focusing on the comfort of the driver.

2.11 Research gap

Even though there has been extensive research on regenerative braking (RB) systems across the world, there is a wide gap when it comes to the availability of such research in the Ethiopian context, indicating an urgent need for research on the topic. The majority of the existing research on the conversion of internal combustion engines to electric motor systems has not taken into consideration the integration of regenerative braking systems, thus affecting the potential efficiency of the systems.

Moreover, there is a lack of simulation techniques specific to the Ethiopian market, which is essential in the optimal design and operation of regenerative braking systems to enable the prediction of performance and detection of design flaws. Furthermore, the benefits of regenerative braking, such as energy savings, longer vehicle mileage, and brake wear, are still not well explored, especially in the case of small electric vehicles in Ethiopia.

Lastly, the literature review has shown that there was a lack of consideration of the local culture and environment, which could have an impact on the effectiveness of such systems, and therefore, it would be very important to focus on the design of such systems in the Ethiopian environment, which takes into account the driving conditions, the traffic, the quality of the roads, etc., to improve the field of electric vehicle conversion in Ethiopia.

CHAPTER THREE

3. RESEARCH METHODOLOGY

3.1 Research Approach and Methodological Framework

This research employs a simulation engineering approach to the design methodology to examine the performance potential of a regenerative braking system, integrated into a converted small Electric Vehicle (EV). The simulation approach has been chosen due to the high costs, safety concerns, and iterative complexities associated with experimental prototyping in the early stages of EV power train development.

The simulation methodology has a top-down approach, starting with the selection of the vehicle, its parameters, the sizing of the power train, the control strategy, and finally the integration of the system. MATLAB/Simulink has been used as the simulation tool of choice, owing to its extensive use in the field of automotive engineering, its ability to model complex multi-domain systems, and the availability of validated component libraries for EVs. The methodology is expressed in flow chart in figure 3.1.

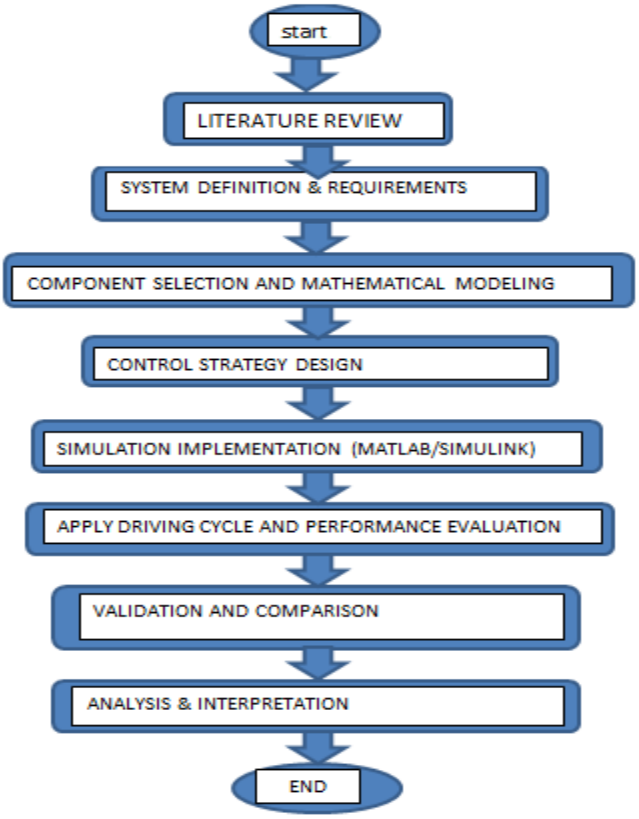

Figure 3.1: Research Methodology Flow chart

3.2 Selection and Characterization of the Baseline Vehicle

3.2.1 Vehicle Selection

In order to select an appropriate vehicle that could be used to implement and test the regenerative braking system, certain parameters were taken into account. The parameters were developed to ensure that the vehicle selected was representative of small passenger cars that were often converted to run on electricity. The selection of the vehicle was also based on the need to have a compact chassis size to allow the integration of the electric motor and the battery pack without having to make significant modifications to the vehicle structure. The parameters were also developed to select a vehicle with a simple mechanical arrangement to avoid complications in

modeling the vehicle and to ensure that the uncertainty of the model was reduced to the lowest possible level.

In addition, the conventional drive train was considered to be an essential requirement to facilitate the implementation of regenerative braking via the driven axle. The operation of the vehicle was to be of an urban nature, characterized by a high frequency of acceleration/deceleration, which would maximize the regenerative braking potential of the vehicle. Lastly, the availability of the vehicle, along with its practical relevance to the EV conversion, was considered to be an essential requirement to ensure that the study reflects the practical scenario of EV conversions.

Considering the various requirements defined in the selection criteria, the Toyota Corolla, with a model year of 1987, was chosen as the base vehicle for this study, as it meets all the requirements set forth by the selection criteria.

3.2.2 Vehicle Parameter Extraction

In order to facilitate the modeling of vehicle dynamics along the longitudinal direction, the vehicle parameters were determined based on the data provided by the vehicle manufacturers, literature values, and estimates for the conversion of the values. The values are then used to determine the total tractive or braking force acting on the vehicle, as given by the equations for vehicle dynamics.

3.3 Power train Design and Component Sizing

The electric power train is tailored to meet specific performance requirements, which are normally dictated by the needs of urban mobility, and at the same time is compatible with the vehicle's energy and structural limitations. This is achieved through the selection of the urban vehicle speed on(0- 90) km/h, which is suitable to cover occasional urban driving and is in the performance envelope of small passenger vehicles.

The grade ability of 5% at was chosen to allow the vehicle to climb moderate grades without exceeding the motor torque limit.

Additionally, the power train is designed for acceptable acceleration performance as well as braking response, taking into consideration the comfort, safety, and regenerative braking performance of the vehicle. The performance targets include the size of the traction motor, the capacity of the battery, as well as the regenerative braking performance, all of which should be within the efficient operating range.

3.3.1 Traction Motor Sizing

The required traction motor power is determined by evaluating the total resistive forces acting on the vehicle:

$$F_{Total} = F_{rolling} + F_{aero} + F_{grade} + F_{acc}$$

Where rolling resistance, aerodynamic drag, and grade forces are calculated using standard formulations. The peak motor power Pmax is then obtained as:

$$P_{max} = \frac{F_{total} * V}{\eta}$$

This approach ensures that the selected motor is capable of meeting worst-case operating conditions without excessive over sizing, which would negatively impact efficiency and cost.

3.3.2 Energy Storage System (ESS) Design

A lithium-ion battery pack was chosen as the energy storage device due to its high energy density, good discharge/charge efficiency, and suitability for the application of regenerative braking. It is designed to operate at a nominal DC bus voltage, which is appropriate for the motor voltage requirements.

The battery capacity is determined through the consideration of several factors: the need to meet the desired urban driving range, which is the ability to complete normal city driving without the

need to recharge the battery frequently; the ability to operate at acceptable depth of discharge levels to prolong the battery's lifespan and avoid over-stressing the battery due to the frequency of the regenerative braking cycles; and the ability to operate at the maximum allowable regenerative charging current, which is limited by the Battery Management System (BMS), to avoid over-current situations during hard regenerative braking cycles.

Moreover, the battery model includes the voltage dynamic and internal resistance characteristics. As such, the simulation can effectively model the behavior of the pack during transient charging and discharging patterns, especially during regenerative braking. This ensures that the ESS is properly sized to meet the demands of the converted electric vehicle.

3.4 Regenerative Braking Architecture

A parallel regenerative braking strategy is adopted, wherein the total braking demand is shared between electrical regenerative torque (T_{reg}) generated by the traction motor and mechanical friction braking torque (T_f), such that the total braking torque is expressed as $T_b = T_{reg} + T_f$

This mode helps in the recovery of the kinetic energy and at the same time ensures the braking performance at all speeds is maintained. There are several critical factors that affect the allocation of the regenerative torque, such as the state of charge (SOC), the maximum allowable charging current as per the Battery Management System, the motor torque-speed characteristics, and the reduced effectiveness of the regenerative torque at low speeds.

To manage this torque distribution intelligently, a fuzzy logic controller (FLC) is employed. The FLC determines the optimal proportion of regenerative and friction braking based on key input variables such as braking demand (or deceleration), vehicle speed, and battery SOC. Using a set of rule-based decisions, the controller increases regenerative torque under favorable conditions such as moderate speeds and acceptable SOC levels while reducing it when constraints arise, such as high SOC (to prevent overcharging), low speeds (where regenerative efficiency is limited), or high braking demand (where friction braking is necessary to ensure safety). The

output of the FLC is the commanded regenerative braking torque with the remaining torque demand fulfilled by the friction braking system.

This control strategy ensures that maximum possible energy is recovered without violating system constraints, while maintaining braking stability, safety, and driver comfort. Additionally, the fuzzy logic approach effectively handles the nonlinear and time-varying nature of the braking system, providing smoother torque transitions compared to conventional linear control methods.

3.5 Control Strategy Development and Comparative Analysis

To regulate regenerative braking torque and optimize energy recovery while maintaining vehicle stability, two control strategies were investigated: a classical Proportional Integral Derivative (PID) controller and a Fuzzy Logic Controller (FLC).

Before the application of the actual vehicle model, the performance of the PID and Fuzzy Logic Controllers was compared and assessed using MATLAB/Simulink to justify the use of the Fuzzy Logic controller to regulate the motor torque. For the PID and Fuzzy Logic Controllers, the step input was applied to the PID and Fuzzy Logic Controllers to control the motor torque. The step input was processed through the PID controller and Fuzzy Logic controller to control the motor torque. The Fuzzy Logic controller processed the same step input through the FLC block with the predefined rule set. The results provided justification for the use of the Fuzzy Logic controller in the regenerative braking simulations.

Comparative analysis for the PID and fuzzy logic controller

The plant model represents the dynamic behavior of the electric drivetrain and its interaction with the control system. It consists of three main components in the forward path: the amplifier, exciter, and motor, each modeled as a first-order transfer function to approximate their respective dynamics. The amplifier represents the power electronics that convert the control signal from the controller into the appropriate voltage and current for the motor, including inherent response delays. The exciter models the actuation dynamics, capturing the transient behavior of the motor input, including inverter and electromagnetic effects, which influence the speed at which the

motor responds to control commands. The motor block itself represents the electromechanical conversion of electrical input into mechanical torque and speed, forming the core of the vehicle's regenerative braking capability. The feedback path includes a sensor dynamics block, which models the response characteristics and measurement delay of speed or torque sensors, providing realistic feedback to the controller. Collectively, this plant model allows for accurate simulation of the system response under both PID and fuzzy logic control strategies.

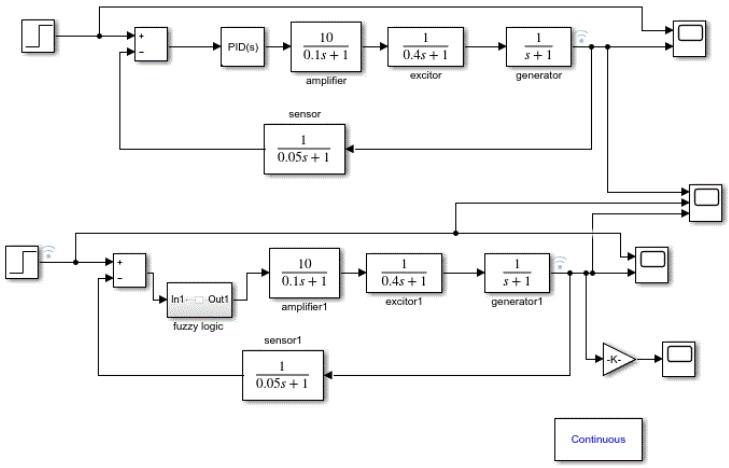

Figure 3. 2: comparative model for PID and Fuzzy logic control

3.5.1 Proportional–Integral–Derivative (PID) Control

A classical PID controller was used to implement the control strategy due to its simplicity and ease of implementation, making it a widely used control strategy in many industrial applications. The control strategy regulates the regenerative torque through constant adjustments to the input to the motor based on the speed error and the driver's brake request. Though the control strategy is effective in linear and well-modeled control applications, it has limitations when used in regenerative braking control due to the non-linear nature of the battery-charging characteristics and the sudden transitions to zero speed from the vehicle deceleration rates.

3.5.2 Fuzzy Logic Control (FLC)

To mitigate the problems identified with the PID controller, the Mamdani-type Fuzzy Logic Controller (FLC) was proposed. The FLC controller depends on linguistic rules based on key variables such as the brake pedal position, vehicle speed, and battery state-of-charge to manage the regenerative torque. To assess and compare the performance of the PID and FLC controllers, a simple signal builder model was created in MATLAB/Simulink to produce step and ramp braking signals to simulate the behavior of the driver.

3.6 System Modeling and Simulation Environment

3.6.1 Subsystem Modeling

The EV and regenerative braking system is implemented by using the MATLAB/Simulink environment, as presented in the following diagram, by using the modular approach, i.e., developing the individual systems independently, as follows:

The battery is represented by using the Thevenin equivalent, while the motor is represented by using the efficiency map-based motor model, as follows:

The vehicle dynamics is represented by the vehicle dynamics model, as follows:

A. Vehicle body

The longitudinal dynamics of the converted electric vehicle, as well as the drive train load, can be characterized by using an integrated model composed of the Vehicle Body (2 Wheel), Simple Gear, and Differential blocks in the Simulink environment. The Vehicle Body block simulates the mass of the vehicle, as well as the effects of the road load, which comprise the inertial, rolling, and aero forces, in a simplified form of a two-wheel configuration to represent the straight-line drive cycle analysis.

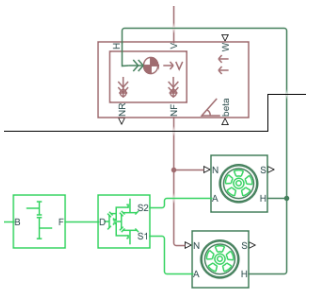

Figure 3. 3: Simplified Vehicle Body Model Used for Simulation

The Differential block distributes the transmitted torque equally to the driven wheels. The physically consistent interaction between the wheels and the electric motor is possible due to this integrated configuration. Using this model, bidirectional energy flow between the wheels and the electric motor can be evaluated realistically for the FTP-75 cycle.

B. Motor block

The traction unit of the vehicle is represented by the DC motor block with separate armature and field excitation control. The DC motor model consists of both electrical and mechanical interfaces. The armature terminals (+A and −A) represent the main electrical input through which current flows to produce electromagnetic torque, while the field terminals (+F and −F) supply the field winding to establish the magnetic flux necessary for torque generation. On the mechanical side, the motor shaft port (M) represents the output through which torque and rotational motion are transmitted to the drivetrain, whereas the load torque (TL) represents the opposing mechanical forces acting on the shaft, including vehicle resistance and braking effects. During regenerative braking operation, the direction of power flow reverses at the armature terminals, allowing the motor to operate as a generator and transfer energy back to the battery. The DC motor can operate in both directions to provide bidirectional torque control. The motor can operate in both motor and generator modes depending on the operating conditions. When the vehicle is subjected to regenerative braking, the load torque applied to the shaft is negative in value. The DC motor operates in the generator mode and converts the mechanical energy available to the motor shaft to electrical energy and feeds it to the battery. The use of the separately excited DC motor model provides an effective representation of the torque and current relationships and the controlled regenerative braking process.

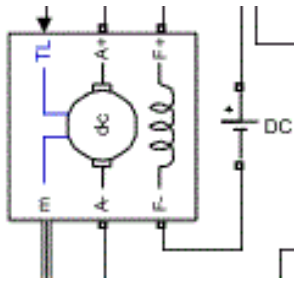

Figure 3. 4: DC Motor Model Used in MATLAB/Simulink

C. fuzzy logic block

A Fuzzy Logic Controller (FLC) block is utilized for the management of regenerative braking torque by making decisions based on different driving conditions. The decision is taken by the controller using the predefined fuzzy inference system (FIS) file, which stores the knowledge about the vehicle's states and the corresponding regenerative braking torque values. The input variables for the FLC represent the different states of the vehicle that occur during regenerative braking like SOC, brake and speed of the vehicle, while the output variable represents the regenerative braking signal sent to the electric motor for smooth transition between motoring and regenerative modes of the vehicle's operation. This type of control is more suitable for regenerative braking because the nonlinearity of the vehicle makes the linear control technique less effective for such conditions.

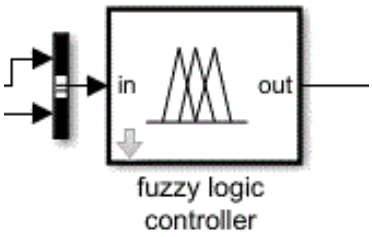

Figure 3. 1: Fuzzy Logic Controller Block Diagram

D. Battery

The energy storage system has been implemented using a Battery block, which simulates the electrical characteristics of the traction battery both during charging and discharging modes of operation. During the course of the simulation, the SOC of the battery has been set to 70% to

represent a more realistic condition, as the SOC of the battery would be close to the maximum value during the simulation, thereby allowing the simulation to account for the regenerative braking conditions without the occurrence of saturation, which would have resulted if the SOC of the battery was set to a maximum value.

The Battery block has been directly interfaced with the electric motor to track the SOC variation of the battery during the course of the FTP-75 drive cycle simulation.

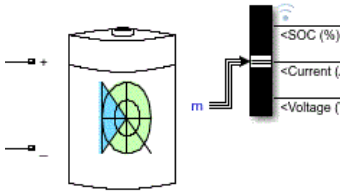

Figure 3. 6: Battery Model Used in MATLAB/Simulink

E. Mosfet and puls generator

The interface between the battery and the DC motor consists of an H-bridge circuit made up of four MOSFET switches to accommodate bidirectional voltage and current flow for both motor and regenerative braking modes.

The Pulse Generator blocks are used to supply control signals to the P-side and N-side MOSFETs to control the H-bridge circuit and prevent shoot-through currents. By varying the duty cycle of the control pulses, the motor armature voltage can be controlled to manage the motor torque during the propulsion mode and to recover the excess energy during the regenerative braking mode.

The simple control strategy is an adequate representation of the DC motor control to evaluate the regenerative braking performance.

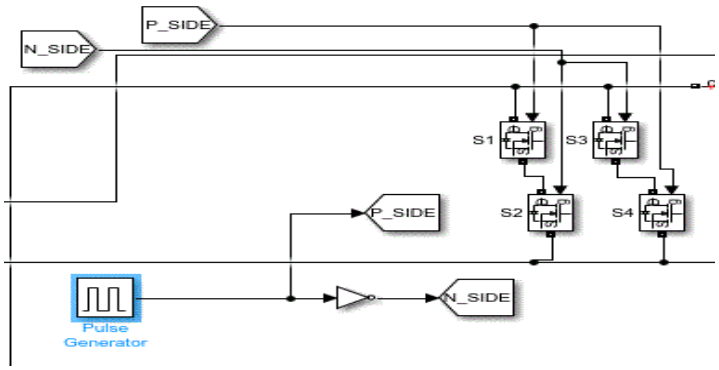

Figure 3. 7: Mosfet and pulse generator model used in matlab/simulink

3.7 regenerative braking matlab model for converted ev

The main simulation model is excited using pre-defined input signals that mimic the driver demand and standard driving scenarios. Step input blocks are used to introduce controlled variations in the accelerator and brake pedal commands, facilitating isolated analysis of the system responses and the controller operation. Furthermore, the FTP-75 driving cycle is used as a time-based reference input signal to mimic realistic urban driving scenarios that involve frequent acceleration and brake events. The use of the FTP-75 cycle allows a fair comparison of the vehicle performance and battery SoC variation when the simulation is carried out with and without the regenerative braking system, such that any observed differences can be attributed to the proposed strategy and not to the input signal variations.

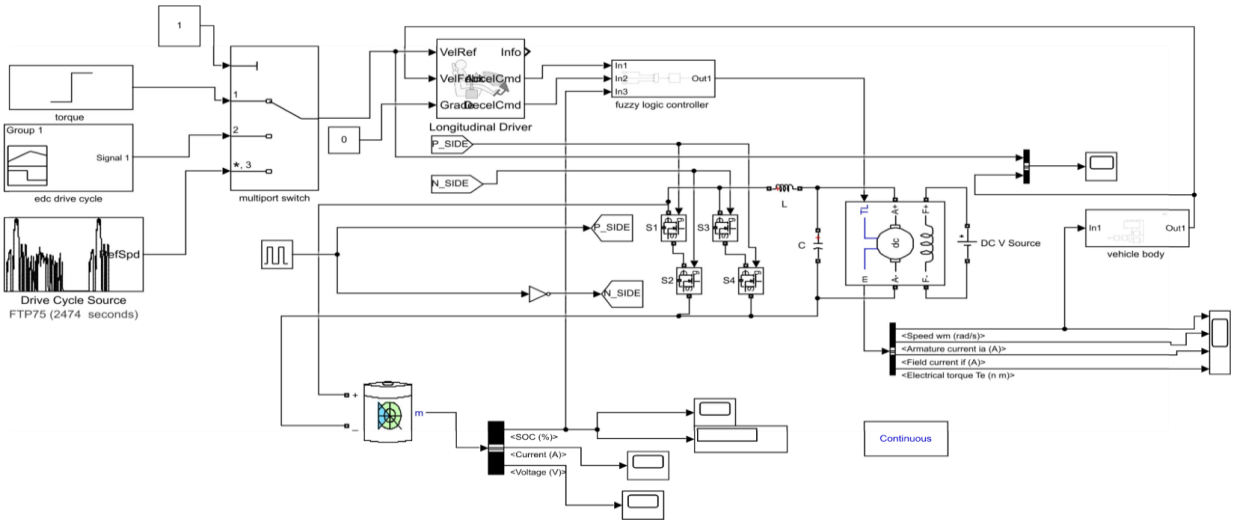

Figure 3. 9: MATLAB/Simulink Model of the Regenerative Braking System for the selected vehicle

3.7.1 Simulation Protocols

The performance of the system was assessed through step input braking tests to evaluate the transient response of the torque and the FTP-75 drive cycle to evaluate the energy consumption and the energy regenerated during the standard driving cycle in the urban area. Suitable solver and controller sample times were chosen to maintain numerical stability in the system.

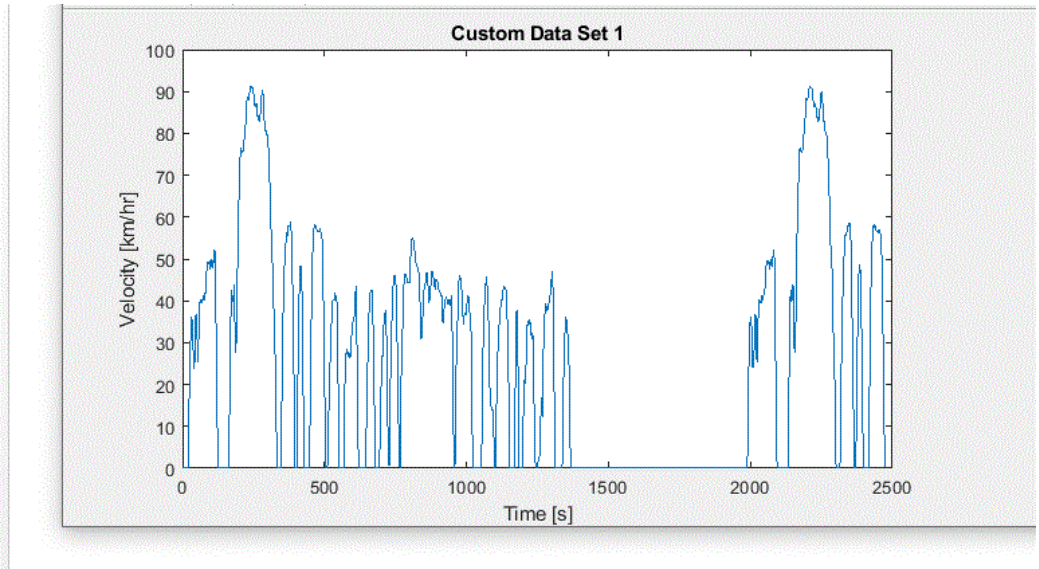

Figure 3. 10: FTP drive cycle used in matlab simulink

3.7 Validation and Performance Evaluation

Analysis of the simulation results and comparison with the results available in the literature on small EV conversions and regenerative braking systems were carried out. The performance was assessed based on the following parameters: regenerative efficiency, expressed as a ratio of the electrical energy regenerated to the total energy used in braking; the SOC profile during the regenerative process; and the energy savings and mileage extension in the regenerative case compared to the non-regenerative case.

This comparison will prove the efficiency of the suggested strategy and the reliability of the simulation model in a real-world driving scenario.

CHAPTER FOUR

4. SYSTEM DESIGN AND REGENERATIVE BRAKING ANALYSIS

4.1 Vehicle Description and Design Parameters

This study was carried out on a converted small passenger vehicle and designed as a fully electric vehicle with the objective of evaluating the design and performance of a regenerative braking system. This vehicle was chosen as a representative vehicle for a class of low-mass electric vehicles designed primarily for urban use cases.

In designing the vehicle, various parameters are defined based on the physical characteristics of the base vehicle, specifications of the electric drive train, and energy storage system and power electronics limitations. In designing the system, various parameters such as vehicle mass, radius of the wheels, gear ratio of the drive train, battery voltage and capacity, and battery charging limits are of significant importance and have a direct impact on the generation of braking force and regenerative torque and maximum recoverable energy during deceleration of the vehicle.

4.1.1 Base Vehicle and Conversion Overview

The base vehicle selected for this study is the Toyota Corolla 1987 model, which was originally designed to use an internal combustion engine but was modified to use an electric motor instead.

The electric motor and motor controller replace the internal combustion engine and the corresponding subsystems. Regenerative braking is achieved by using the electric motor in generator mode during vehicle deceleration to convert the vehicle's kinetic energy back to electrical energy and store it in the battery, depending on the current capacity of the battery management system. Mechanical friction brakes can also be used to provide safe braking during high deceleration demands and low-speed operation.

Figure 4. 1: Toyota corolla 1987 (Kemezor, n.d).

4.1.2 Key Vehicle Parameters

The essential vehicle parameters needed to analyze the regenerative braking are listed in Table 4.1, which will be used to calculate the theoretically available maximum kinetic energy as well as the losses due to rolling resistance and aerodynamic drag.

The parameters listed will be used as input to the vehicle dynamic modeling, which will be used to calculate the resisting forces, braking force distribution, regenerative braking, etc., of the vehicle. The geometric parameters of the vehicle, such as the radius of the wheels, distance of the axles, etc., have been listed to aid the analysis of the vehicle dynamics.

Table 4. 1: presents the assumed vehicle parameters used throughout the analysis

Parameter	**Value (Unit)**
Curb Weight	850 kg
Frontal Area	1.9 m^2
Aerodynamic Drag Coefficient	0.38
Wheel Radius	0.29 m
Distance from CG to Rear Axle (Lr)	1.2 m
Distance from CG to Front Axle (Lf)	1.0 m
Wheelbase (L)	2.2 m

4.1.3 Converted Vehicle Mass Determination

The original vehicle mass before conversion is: m original=850 kg, and considering an 11.5% increase in weight due to retrofitting according the (Duangtongsuk et al. (2022))

M converted = m original × (1+0.115) m

M converted = 850×1.115 m

M converted = 947.75 kg ≈ **950 kg**

4.2 Acting Forces During Vehicle Motion

i. **Uniform Horizontal Motion**

During uniform motion on a horizontal road, the traction force generated by the driving wheels (Fw) must balance all resistive forces opposing the vehicle's motion. This ensures steady velocity without acceleration. Mathematically, this relationship expressed as**:**

$$F_w = F_t$$

The total resistance force (Ft) that the vehicle must overcome during uniform horizontal motion is the sum of the rolling resistance force (Fr) and the aerodynamic drag force (F_d):

$$F_t = F_r + F_d, \qquad \text{for slope=0, } F_i=0$$

ii. **Rolling Resistance Force**

The rolling resistance force (Fr) depends on the resistance coefficient of the road surface (f_0) and the vehicle's weight. Coefficient of Rolling Resistance taken 0.012

The rolling resistance can be calculated as:

$$F_r = f \times G$$

$$= f_0 \times m \times g,$$

$= 0.012 \times 950 \times 9.81$

$=111.8$ N

iii. Aerodynamic Drag Force

The aerodynamic drag force (F_d) arises due to the air resistance opposing the motion of the vehicle. It depends on the vehicle's shape, frontal area, air density, and speed.

The force is calculated using:

$$F_d = \frac{\mathrm{Cd} \times \rho \times \mathrm{S} \times V^2}{2}$$

$$= \frac{0.38 \times 1.22 \times 1.95 \times 193}{2}$$

$=87.24$N

This aerodynamic force increases with the square of the vehicle speed, meaning it becomes more significant at higher speeds. It represents the energy the vehicle must overcome to maintain motion through the air.

iv. Climbing a Slope

When a vehicle climbs a road with an incline, an additional resistance force due to gravity called the grade resistance or slope resistance acts opposite to the direction of motion. This force depends on the vehicle mass, gravitational acceleration, and the slope angle.

The slope resistance force is given by:

$$F_i = G \times sin$$

$= m \times g \times \sin\alpha$

$=950 \times 9.81 \times \sin 2.86$

$=463$ N

A 5% road slope corresponds to an inclination angle of approximately 2.86°.

The vehicle must generate an additional 463 N of traction force just to overcome gravity when climbing a 5% slope. This significantly increases energy consumption and reduces the amount of energy that can be recovered during regenerative braking on uphill segments.

v. Acceleration Resistance (Inertial Force) When the vehicle accelerates, an additional force is required to increase its speed from the initial velocity Vinitial to the final velocity Vfinal. This acceleration force is determined using Newton's Second Law.

F= m ×a, but, $a = \frac{(V_{final} - V_{initial})}{t}$

$$= \frac{(13.89 - 0)}{7}$$

=1.984 m/s2

Therefore F=950×1.984

F= 1884.8 N

The vehicle requires 1884 N of additional traction force to accelerate from zero to 50 km/h (13.89 m/s) in 7 seconds.

Total Required Traction Force (Steady State Climbing)

During vehicle motion, the driving wheels must generate enough traction force Fw to overcome all acting resistances. Since no acceleration is considered here, the required traction force equals the total resistance force:

$$F_w = F_t$$

$$F_t = F_r + F_d + F_i$$

$$= 111.8 + 87.24 + 490$$

$$= 690\text{N}$$

4.3 Required Power at the Wheels

I. Required Power at the Wheels (Steady-State)

The mechanical power needed at the driving wheels is determined from the total resistance force and vehicle speed:

$$P_w = \frac{F_w \times V}{3.6} = \frac{F_t \times V}{3.6}$$

$$= \frac{690 \times 50 \text{ km/h}}{3.6}$$

$$= 9584w = 9.58 \text{ KW}$$

Total Tractive Force under Acceleration on Level Road

The vehicle needs approximately 9.58 kW of power at the wheels to maintain a speed of 50 km/h on a 5% slope, overcoming rolling resistance, aerodynamic drag, and gravitational slope force.

$$F_{total} = F_a + F_r + F_d$$

$$= 1884.8 + 117.72 + 87.24$$

$$= 2089.76N$$

II. Motor Power Requirement (Worst-Case Condition)

The motor power estimation is based on the total tractive force that is required for the movement of the vehicle under combined driving conditions. After calculating the rolling resistance, aerodynamic drag, slope resistance, and acceleration force, the total required traction force was calculated by summing all the individual tractive forces that act on the vehicle's wheels. The total force is then multiplied by the vehicle's speed to obtain the power requirement for the motor.

$$P_{motor} = F_{total} \times v$$

$$= 2089.76N \times 13.889$$

$$= 29KW$$

In this particular case, it was determined that the total driving force was 2089.6 N, and at a speed of 13.89 m/s or 50 km/h, the power required by the motor will be approximately 30 kW. This power value

represents a peak value of power required by the motor at any given time while accelerating on a 5% slope. It should be noted that it is important in determining the type of motor and battery pack required by a vehicle.

4.4 Assumptions for Energy Consumption and Driving Range

To properly size the battery and estimate the required energy capacity for the converted electric vehicle (EV), several assumptions are made based on regulatory requirements and practical design targets.

4.4.1 Regulatory Requirements

According to the Ethiopian standard ES 7073:2023, any retrofitted electric vehicle must achieve a minimum driving range of 200 km per full charge**.** The same standard stipulates that energy consumption of the vehicle must not be less than 4.0 km per kWh of stored energy**.**

4.4.2 Design Assumptions

With the small EV, which is based on an ICE vehicle, the assumed energy consumption for the vehicle is 10-15 kWh/100km, taking into consideration the mass of the vehicle, aerodynamic resistance, electric drive train, as well as driving behavior.

The average vehicle speed is assumed to be 50km/h, or approximately 13.89 m/s, as the driving conditions for the vehicle are assumed to be urban, as will be considered later for energy and power calculations.

4.4.3 Assumptions for average power consumption under nominal driving condition

The energy consumption *E* per 100 km determined by the formula:

E= P_{el}.100/V

Eper meter= $\frac{10\ \text{kWh} \times 3.6 \times 106\ \text{J/kWh}}{100{,}000} = 360\ \text{J/m}$

Electric power used by the vehicle is given by

$$P_{el} = \frac{E \times V}{100}$$

$$= (360\ \text{J/m} \times 13.33)$$

$$= 4.8\ \text{Kw}$$

This represents the average power consumption under nominal driving conditions.

4.4.4 Minimum Usable Battery Capacity

The vehicle will travel more than 200 km range (CB) so, the usable battery capacity (S) can be calculated using the expression:

$$\text{Minimum usable battery capacity} = \frac{\text{driving range} \times \text{energy consumption}}{100}$$

$$= \frac{200 \times 10}{100}$$

$$= 20\ \text{kWh}$$

While the calculated minimum battery capacity required to achieve the desired minimum range of 200 km is 20 kWh, assuming an energy consumption rate of 10 kWh/100 km, a larger battery capacity is used to account for real-world driving scenarios, energy loss, and battery degradation.

4.5 Kinetic Energy and Regenerative Braking Potential

The kinetic energy of a moving vehicle represents the total mechanical energy available in motion, which can be recovered during braking. It is expressed by the classical equation:

$$E_K = {}^1\!/_2\ mv^2$$

For the selected test vehicle with a gross mass of 950 kg, the kinetic energy values are calculated for various deceleration events corresponding to vehicle speeds ranging from 90 km/h to 10 km/h. The calculated values are presented in Table 4.2.

4.5.1 Kinetic energy available for recovery

$$E_k = \frac{1}{2} m\left(v_i^2 - v_f^2\right)$$

At a speed of **50 km/h-0**, the vehicle has a kinetic energy given by:

$$E_K = {}^1/_2\ mv^2$$

$$=½\times 950\times(13.89)^2$$

$$= 91{,}652\text{J}$$

At 50 km/h, the converted EV stores about 91.7 kJ of kinetic energy. This energy represents the total amount of motion-based energy that the vehicle possesses before braking. During regenerative braking, a portion of this kinetic energy will be converted back into electrical energy by the traction motor operating as a generator. However, the actual recoverable energy will be lower.

4.5.2 Recoverable energy considering system efficiency

$$E_{regen} = E_k \times \eta_{regen}$$

$$\eta_{regen} = \eta_{motor} \times \eta_{controller} \times \eta_{battery}$$

$$= 0.85 \times 0.95 \times 0.9$$

$$=72\%$$

So, $$E_{regen} = 72\% \times 91.7 \text{ kJ}$$

$$= 66 \text{ kJ}$$

This means that braking from 50 km/h to 10 can theoretically return about 66 kJ to the battery, helping extend driving range and reduce the load on mechanical brakes.

Here's the kinetic energy table for 950 kg vehicle decelerating from various speeds down to 10 km/h:

Table 4. 2: Kinetic energy of the vehicle at different velocities

Speed (km/h)	**Speed (m/s)**	$E_{kinetic}(J)$	$E_{kinetic}(KJ)$
90	25.00	293,700	294
80	22.22	230,600	231
70	19.44	175,900	176
60	16.67	128,300	128
50	13.89	87,900	88
40	11.11	55,000	55
30	8.33	29,300	29
20	5.56	11,000	11

As depicted in the figure, the kinetic energy increases in a proportional relationship to the square of the vehicle's velocity. The depicted relationship emphasizes the fact that a slight increase in the vehicle's speed results in a considerable increase in the energy levels. For example, the energy at a speed of 90 km/h is more than eight times greater than the energy at a speed of 30 km/h.

This stored kinetic energy is the potential energy available for recovery using regenerative braking. However, the amount of energy that can be recuperated using the regenerative system depends on the efficiency of the system, while the energy lost is a result of friction and inefficiencies in the system.

4.5.3 Classification of Deceleration Levels

For the analysis of braking and regenerative braking performance, three deceleration levels are defined based on typical vehicle operation and safety considerations. These levels are used

throughout Chapter 4 to evaluate braking force demand, stopping distance, and the contribution of the regenerative braking system.

i. Gentle Braking (a=1–3 m/s2)

Gentle braking corresponds to low deceleration levels commonly encountered during routine driving, such as approaching intersections, minor speed adjustments, or low-traffic urban conditions. This deceleration range prioritizes passenger comfort and vehicle stability.

ii. Moderate Braking (a=4–6 m/s2)

Moderate braking occurs when a faster reduction in vehicle speed is required, such as during typical urban traffic maneuvers or controlled deceleration from higher speeds. This deceleration range produces noticeable but manageable longitudinal load transfer.

iii. Aggressive Braking (a=7–9 m/s2)

Aggressive braking represents near-emergency or emergency stopping conditions where maximum deceleration is required for safety. These deceleration levels approach the adhesion limits of the tire–road interface.

In this case, the braking force requirement is far higher than the regenerative capacity of the electric power train. The motor torque limits, as well as the battery current acceptance limits, play a crucial role in the restriction of regenerative braking, thus making the friction brakes the main form of braking action. The regenerative braking is minimal and of lesser importance compared to the vehicle's safety.

4.5.4 Required braking force

To determine the braking force required during vehicle deceleration, a uniform deceleration assumption adopted. The vehicle assumed to decelerate on a horizontal road, but resistive forces

such as aerodynamic drag and rolling resistance are neglected for simplicity, as the braking force dominates during deceleration.

From basic kinematic relations, the braking force required to decelerate a vehicle from an initial velocity vi to a final velocity vf over a braking distance d is given by:

$$F_b = \frac{m \cdot (v_i^2 - v_f^2)}{2d} = ma$$

$$d = \frac{(v_i^2 - v_f^2)}{2a}$$

This braking force represents the total force required at the wheels, which later distributed between regenerative braking and the mechanical braking system based on system limitations.

4.5.5 Braking Force at Different Deceleration Levels

The total braking force required at the wheels calculated using Newton's second law:

$$F_b = ma$$

For the converted Volkswagen Beetle with a mass of m=950 kg, braking forces corresponding to different deceleration levels calculated as follows:

Gentle braking ($a = 3\ (\mathrm{m/s^2})$

$$F_b = 950 \times 3 = 2850\ N$$

Moderate braking ($a = 6\ (\mathrm{m/s^2})$

$$F_b = 950 \times 6 = 5700\ N$$

Aggressive braking ($a = 9\ (\mathrm{m/s^2})$

$$F_b = 950 \times 9 = 8550\ N$$

Table 4. 3: Relationship between deceleration and braking force

Deceleration(m/s²)	Braking force (N)
3	2850 N
6	5700 N

9	8550 N

The braking force increases linearly with deceleration. A gentle deceleration of 3 m/s² requires approximately 2.85 KN, while an aggressive deceleration of 9 m/s² demands about 8.55 KN of total braking force.

This relationship is of prime importance to assess the effectiveness of the regenerative braking system. Under light braking conditions, the regenerative braking system can be utilized to a higher extent, as the braking force can be supplied by the electric motor itself. But, in the case of moderate and severe braking conditions, the motor torque as well as the charging current of the batteries limits the regenerative braking system, making the use of the mechanical friction brakes more prominent.

4.5.6 Stopping Distance at Different Deceleration Levels

The stopping distance is calculated assuming constant deceleration using the kinematic relation:

$$d = \frac{V^2}{2a}$$

At 50km/hr at gentle braking the stopping distance will be

$$d = \frac{13.89^2}{6} = 32.2\,m$$

Table 4. 4: Stopping Distance at Different Speeds and Deceleration Levels

Speed (km/h)	Velocity (m/s)	d @ a=3 m/s²	d @ a=6 m/s²	d @ a=9 m/s²
90	25.00	104.2m	52.1m	34.7m
80	22.22	82.3m	41.2m	27.4m
70	19.44	63.0m	31.5m	21.0m
60	16.67	46.3m	23.2m	15.4m
50	13.89	32.2m	16.1m	10.7m
40	11.11	20.6m	10.3m	6.9m
30	8.33	11.6m	5.8m	3.9m

20	5.56	5.1m	2.6m	1.7m
10	2.78	1.3m	0.6m	0.4m

The stopping distance decreases sharply as the deceleration rate increases. For instance, at 90 km/h, the vehicle requires approximately 104 m to stop under gentle braking (3 m/s²), but only 35 m under aggressive braking (9 m/s²). This relationship illustrates that braking performance improves with higher deceleration;

4.6 Motor-Generator Performance Model

The traction motor used in the converted Volkswagen Beetle operates as both a motor during propulsion and a generator during regenerative braking. The same torque–speed and power limits apply in both modes, with the direction of power flow reversed during regeneration.

4.6.1 Motor Torque-power Characteristics

The motor operation is constrained by two primary limits: a continuous (rated) limit and a short-term (peak) limit.

Continuous (Rated) operation:

The continuous rated power of the motor is 30 kW and at torque of;

$$T_{rated} = 80\ N.m$$

This region defines the allowable operating condition for sustained operation without excessive thermal stress. In regenerative mode, this limit represents the maximum continuous braking torque that can be applied electrically.

Short-Term (Peak) operation:

The short-term maximum power is 45 kW. This represents the peak regenerative capability during brief acceleration or braking events.

$$T_{peak} = 126\ N \cdot m$$

When the product of torque and speed exceeds this limit, the motor operates in a power-limited region, and the torque is reduced accordingly to prevent exceeding the maximum allowable power.

4.6.2 Shaft Power Calculation

The mechanical output power of the traction motor is calculated using the standard rotational power formula:

$$P_{shaft}(\text{kW}) = \frac{\text{T (N} \times \text{n (rpm))}}{9550}$$

$$Max\ P_{shaft}(\text{kW}) = \frac{(80 \times 3411)}{9550}$$

$$= 45kw$$

At a motor speed of approximately $2984\ rpm$, a torque of $80\ N \cdot m$ produces a shaft power of $30\ kW$ corresponding to the continuous rated operating point.

At higher speeds, application of the peak torque would result in shaft power exceeding $45\ kW$; therefore, the shaft power capped at this value, defining the maximum regenerative and traction power capability of the motor.

4.6.3 Regenerative Power Delivered to the Battery

Not all mechanical power generated during regenerative braking is stored in the battery due to conversion losses. The effective electrical power delivered to the battery calculated as:

$$P_{batt} = P_{shaft} \times \eta_{con} \times \eta_{batt}$$

$$= P_{shaft} \times 0.95 \times 0.85$$

$$= P_{shaft} \times 0.8$$

Thus, approximately 80% of the mechanical regenerative power converted into usable electrical energy and stored in the battery.

Table 4. 5: power output shaft and battery

$n\ (rpm)$	$P_{shaft}\ at\ T = 80$	$P_{batt}\ @\ T = 80$	$P_{shaft}\ @\ T = 126$	$P_{batt} @\ T = 126$
1000	8.38	6.70	13.19	10.55
2000	16.75	13.40	26.38	21.10
2984	25.00	20.00	39.36	31.49
3200	26.81	21.45	42.22	33.78
3410	28.54	22.83	45 capped	36.00
4000	33.51	26.81	45	36.00
5000	41.89	33.51	45	36.00
6500	54.45 capped	43.56	45	36.00

The table highlights how power output varies with speed and torque, which is essential for sizing the motor, inverter, and battery for efficient energy recovery during regenerative braking in electric vehicle conversions.

At T = 80 N.m, the shaft power increases linearly with the motor speed and reaches 30 kW at the base speed of 2984 rpm. However, the electrical power supplied to the battery is proportionally less due to efficiency losses. When the torque is set to 126 N.m, the shaft power available is well above 45 kW at higher speeds; thus, the motor continuous power rating is used to limit the shaft power. This shows the significance of controlling the motor torque/power at higher speeds to prevent motor overload and battery overload during regenerative braking.

4.6.4 Maximum Regenerative Torque Capability

The maximum regenerative braking torque produced by the traction motor is constrained by both torque limits and shaft power limits. These constraints define the allowable regenerative torque as a function of motor speed.

Regenerative Torque Limits

The motor characterized by:

Peak and Continuous torque limit: $T_{peak} = 126N\ peak\ and\ T_{cont} = 80Nm$ continous

Peak and rated shaft power of the motor is limited to; $P_{peak} = 45\ kW$ and $P_{cont} = 30kW$

Peak shaft power, $C_{\ peak} = P_{peak} \times 9550$

$= 429, 750$

Continuous (rated) shaft power, $C_{cont.} = P_{cont} \times 9550$

$= 238, 750$

Then the maximum available regenerative torque $(N.m)$ is:

Short-term (peak) regen torque at 3200

$T_{regen\ peak\ (n)} = \min(126, \frac{C_{peak}}{\omega} = \frac{429750}{\omega})$

$= \frac{429750}{3200}$

= 134Nm but limited 126Nm

At 3200 rpm, peak regenerative torque is still torque-limited, not power-limited.

Continuous (sustained) regen torque

$$T_{regen\ cont\ (n)} = \min(80, \frac{C_{cont}}{\omega} = \frac{238750}{\omega})$$

$$= \frac{238750}{3200}$$

$$= 74.6 \text{ Nm}$$

Calculate Regenerative Power at Motor Shaft

$$P_{motor\ regen} = \frac{(T_{regen} \times \text{n})}{9550}$$

$$P_{motor\ regen} = T_{regen} \times \omega$$

$$= 126 \times 3200$$

$$= 40\ kw$$

Below the 45kW peak limit is allowed.

Table 4. 6: Regenerative Torque and Power Limits at Different Motor Speeds

Motor Speed (rpm)	$T_{regen,cont}$ $(N.m)$	$P_{regen,cont}$ (kW)	$T_{regen,peak}$ (Nm)	$P_{regen,peak}$ (kW)
1000	80	8.38	126	13.2
2000	80	16.7	126	26.4
2984.38	80	30	126	39.3
3200	74.61	30	126	42.2
3410.71	69.98	30	126	45
4000	59.69	30	107.44	45
5000	47.75	30	85.95	45
6500	36.81	30	66.12	45

The table indicates the regenerative braking torque the motor can utilize at different speeds under both continuous (80 N·m) and peak (126 N·m) conditions. The motor can utilize its maximum regenerative braking torque at low speeds because the power is well within the limits. As the speed of the motor rises, the regenerative braking torque must be limited to keep the motor's power below the maximum allowable, both under continuous (30 kW) and peak (45 kW)

conditions. This explains the falling continuous torque after 3000 rpm, as well as the falling peak torque after 4000 rpm, as shown in the table above.

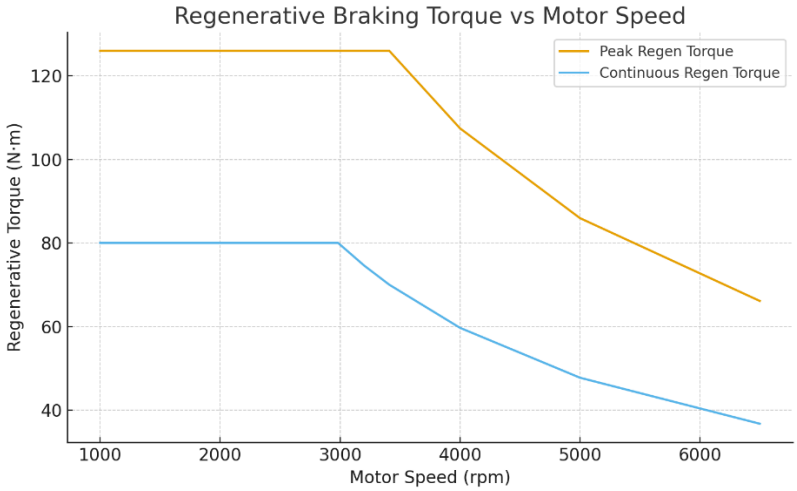

Figure 4. 2: Regenerative Braking Torque Vs Motor speed

4.7 Regenerative Braking Torque and Wheel braking Force

The regenerative braking torque produced by the traction motor is transmitted to the driven wheels through the drive train, resulting in a tangential braking force at the tire–road interface. This force determines the vehicle deceleration achievable through regenerative braking.

$$T_{regen} = F_{regen} \times r_w$$

$$F_{regen} = \frac{T_{regen}}{r_w}$$

Where r_w is the effective wheel radius (m).

A larger wheel radius reduces the available braking force for the same torque, while a smaller wheel radius increases it. This relationship is fundamental in EV regenerative braking analysis and is widely used in electric vehicle dynamics.

4.7.1 Motor Torque to Wheel Torque conversion

When the motor produces regenerative torque, that torque is transmitted to the wheels through the drive train. Because the motor usually spins much faster than the wheels, the gearbox and final-drive increase the torque before it reaches the wheels. The wheel torque is given by:

Wheel torque:

$$T_w = \frac{T_{motor,regen} \times \text{ig} \times \eta\text{td})}{\text{Nw}}$$

$$T_w = \frac{(126\ \text{Nm} \times 13 \times 0.90)}{1}$$

$$= 1474.2\text{Nm}$$

Braking force at each wheel:

$$T_w = \frac{T_{\text{axle, total}}}{\text{Nw}}$$

$$= \frac{1474.2\text{Nm}}{2}$$

$$= 737\text{N}$$

4.7.2 Regenerative Braking Force at the Wheels

The tangential braking force at each wheel is calculated as:

$$F_w = \frac{T_w}{r_w}$$

$$F_w = \frac{737}{0.29}$$

$$= 2541.7\ \text{N PER WHEEL}$$

4.7.3 Vehicle Deceleration Due to Regenerative Braking

The resulting vehicle deceleration achievable through regenerative braking alone is:

Total regenerative braking force at the road (both driven wheels):

$$F_{\text{regen,total}} = 2 \times F_w$$
$$= 2 \times 2541$$
$$= 5083\text{N}$$

This is the total braking force applied at the road due to regenerative braking alone.

Resulting vehicle deceleration from regenerative alone:

$$\text{aregen} = \frac{F_{regen,total}}{m}$$
$$\text{aregen} = \frac{5083}{950}$$
$$= 5.35\ \text{m/s}^2$$

Deceleration as fraction of g:

$$\frac{\text{aregen}}{g} = \frac{6.35}{9.81}$$
$$= 0.6$$

Table 4. 7: Regenerative Deceleration for Different Regenerative Torques

Motor Regen Torque (Nm)	Axle Torque (Nm)	Torque per Wheel (Nm)	Force per Wheel (N)	Total Braking Force (N)	Deceleration (m/s^2)
126 Nm	1750	875	3017	6034	6.35
100 Nm	1386	693	2390	4780	5.03
80 Nm	1108	554	1912	3824	4.02
60 Nm	831	416	1437	2874	3.02
40 Nm	554	277	955	1910	2.01
20 Nm	277	138	477	954	1.00

This is illustrated in the table below, showing the direct proportion that the vehicle's deceleration increases in accordance with the regenerative motor torque values. The lower regen torque values, ranging from 20 to 40 Nm, provide mild braking forces in the range of 1.0 to 2.0 m/s², which is the extent to which the vehicle is slowed down in everyday life. The medium regen torque values, ranging from 60 to 80 Nm, provide a moderate braking force in the range of 3.0 to 4.0 m/s², which is the maximum that can be achieved in a normal vehicle setup. The peak values, ranging from 100 to 126 Nm, mathematically provide a high decelerating force that exceeds 5.0 m/s², though this is purely theoretical and exceed what the battery, converter, and motor would safely sustain in real regenerative operation.

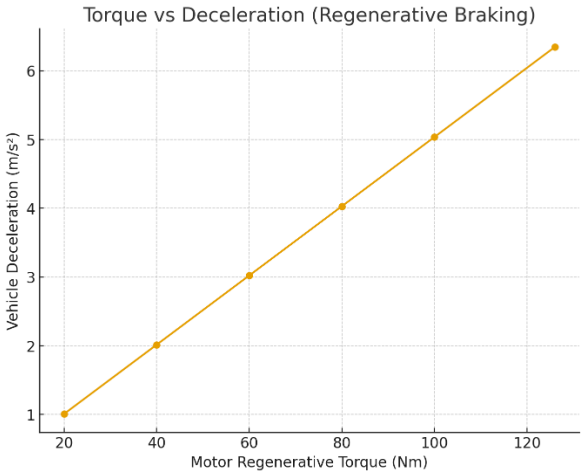

Figure 4. 3: torque Vs deceleration (regenerative braking)

The graph shows the linear relationship between regenerative torque and vehicle deceleration, as the more the regenerative torque, the higher the vehicle deceleration. The linear relationship shows the sensitivity of the braking performance as an increase in regenerative torque produces a considerable increase in braking force.

4.7.4 Tire–Road Friction Limitation on Regenerative Braking

The maximum usable braking force at the wheels is limited by the tire–road friction. If the braking force exceeds the available tire adhesion, wheel slip occurs and the braking force must be reduced through control intervention.

For dry asphalt, the coefficient of friction typically lies in the range 0.7–1.0. In this study, a conservative value of μ=0.8

The maximum friction-limited braking force is given by:

$$F_{max,tire} \leq \mu m g$$

$$F_{max,tire} = \mu \times m \times g$$

$$= 0.8 \times 950 \times 9.81$$

$$= 7455.6N$$

Tire adhesion (safety) check

From the regenerative braking analysis: $F_{regen,total} = 5084\ N$

Since $F_{regen,total} < F_{max,tire}$

$$5084N < 7455.6N$$

the regenerative braking force does not exceed the tire–road friction limit. Therefore, under dry asphalt conditions, regenerative braking alone will not cause wheel slip.

If the regenerative braking demand were to exceed the available tire adhesion, wheel slip would occur and regenerative torque would be reduced by the motor controller and with additional braking provided by the mechanical friction brakes.

4.7.5 Electrical power generated

The vehicle speed first converted to wheel angular speed. For a vehicle speed of 50 km/h:

$$\omega = \frac{v}{r_w},$$

First, convert km/h to m/s $= \frac{V\ (\text{km}/\text{h})}{3.6}$

$$= \frac{50\ \frac{\text{km}}{\text{h}}}{3.6}$$

$$= 13.89\text{m/s}$$

Wheel angular speed

To compute ω from vehicle speed v (m/s):

$$\omega = \frac{V}{r_w}$$

$$= \frac{13.89}{0.29}$$

$$= 48\ rad/s$$

Electrical power generated

Motor angular speed obtained using the overall gear ratio $ig = 13$

$$\omega_{motor} = ig \times \omega_{wheel}$$

$$= 13 \times 47.9$$

$$= 622.7\ rad/s$$

Mechanical Power at the Motor Shaft

Mechanical regenerative power at the motor shaft is:

$$P_{shaft} = T_{regen} \times \omega_{motor}$$

For typical regenerative torque values:

At 40Nm, $P_{shaft} = 40 \times 622.7$

=24.9kw

At 60Nm, $P_{shaft} = 60 \times 622.7$

=37.4kw

Electrical power delivered to the battery

Accounting for inverter and battery charging efficiencies

$$P_{batt} = P_{shaft} \times \eta_{con} \times \eta_{batt}$$

$$= P_{shaft} \times 0.855$$

At 40Nm, $P_{batt} = 24.9 \times 0.855$

=21.3 kW

At 60Nm, $P_{batt} = 3\,7.4 \times 0.855$

= 32 kW

Battery charging current

With battery voltage $V_{batt} = 250\,V$

$$I_{batt} = \frac{P_{batt}}{V_{batt}}$$

At 40 Nm**:** $I_{batt} = \frac{21{,}300}{250} = 85.2\,A$

At 60 Nm $I_{batt} = \frac{32{,}000}{250} = 128\,A$

Table 4. 8: mechanical power of shaft and electrical power delivered to the battery at different speed at 40N

Speed (km/h)	P_{shaft}(W)	P_{batt}(W)	$I_{delivered}$(A)
10	124.5	5.0	4.3
20	249.0	10.0	8.6
30	373.5	14.9	12.7
40	498.1	19.9	17.0
50	622.7	24.9	21.3
60	747.2	29.9	25.6
70	871.7	34.9	29.8

80	996.3	39.9	34.1
90	1120.8	44.8	38.3
100	1245.4	49.8	42.6

As vehicle speed increases, regenerative power rises linearly due to increasing motor speed. At moderate speeds (below 50 km/h), the battery charging current remains within the BMS limit.

4.8 Battery and Energy Storage Capacity Verification

Proper sizing of the battery pack is essential to ensure that regenerated braking energy can be absorbed safely without exceeding voltage, current, or thermal limits. In this section, the battery capacity verified against the energy recovered during a representative braking event.

The nominal energy capacity of the battery pack is given by:

$$E_{batt} = V_{batt} \times Q$$
$$= 300\text{V} \times 100Ah$$
$$= 30\text{KWh}$$

To preserve battery life and prevent overcharging, only a fraction of the nominal capacity is usable. Assuming a usable depth of discharge of 90%

$$E_{batt,usable} = 0.85 \times 30kwh$$
$$= 25.5kWh$$

4.8.1 Energy Recovered During a Single Braking Event

Then Compute Energy Recovered during One Braking Event braking from 50 km/h to 10 km/h over 20 seconds**.**

$$E_{regen} = P_{batt} \times t$$
$$= 21.3 \times 20$$
$$= 213\text{kJ}$$

Convert Joules to Watt-hours: $E_{regen} = \frac{213{,}000\,J}{3600}$

$$= 59.2Wh$$

If we assume 100 braking events so, $E_{regen,total} = 100 \times 59.2Wh$

$$= 5920Wh$$

4.8.2 Battery Capacity Adequacy Check

The usable battery energy is $E_{batt} = 25000\ wh$

so clearly:

$$E_{regen} \leq E_{batt}$$

This shows that the capacity of the batteries to store energy is more than enough to store the regenerative energy from a realistic braking scenario. In the case of 100 moderate braking scenarios in a 200 km drive, the vehicle will be able to regenerate 5.9 kWh of energy, which is only 26% of the available capacity of the batteries (25.5 kWh). This shows that regenerative braking can be an effective tool in the efficiency of the vehicle without overloading the capacity of the batteries.

4.8.3 Maximum Charge Power

$$P_{batt,charge,max} = V_{pack} \times I_{charge,max}$$

$$= 300 \times 90$$

$$= 27{,}000\ W = 27\ kW$$

The BMS will limit the charging current to 90 A to protect the battery. The controller will automatically reduce regen torque to ensure the battery is not overloaded.

$$I_{charge,max} = Charge\ C\ rate \times Battery\ Capacity\ (Ah)$$

$$= 0.9 \times 100Ah$$

$$= 90Ah$$

If you maintain regen for 10 seconds, the recovered energy is

$$E = P \times t$$

$$= 27000 \times 10$$

$$= 270{,}000\,J \;=\; 62.5Wh$$

So in a 10 s braking event, your system could return about 62.5Wh to the battery.

This represents the maximum energy that can be safely stored during a single braking event under the BMS current limit. In practice, the actual recovered energy may be slightly lower, depending on vehicle speed, motor torque, and average regenerative power during braking.

4.8.4 State of Charge (SOC) Limitation regenerative braking

The SOC also plays an important role in the limitation of the regenerative braking ability. When the SOC is too high, the battery can get overcharged, and when the SOC is too low, the battery can get undercharged. Therefore, the Battery Management System (BMS) controls the amount of current available for regenerative braking.

When the SOC is within the normal range (15 to 85 percent), the battery can accept the maximum allowable current for regenerative braking.

SOC Dependent Charge Current Model

The effective regenerative charging current modeled as:

$$I_{charge\ effective}(SOC) = I_{charge,max} \times f\ (SOC)$$

$$\text{F (SOC)} = \int_0^0 \frac{(SOC-15)}{70} \qquad \begin{matrix} \text{SOC} \le 15\% \\ 15\% < \text{SOC} < 85\% \\ SOC \ge 85\% \end{matrix}$$

1. SOC ≥85% charging not allowed
2. SOC at 50% $\qquad f(50) = \frac{50-15}{70} = 0.5$

$$I_{eff} = 90 \times 0.5 = 45\ A$$

3. SOC = ≤15% charging not allowed

Even though the electric motor may be capable of producing significant regenerative torque, the actual regenerative braking power is limited due to the battery-charging limitations that depend on the SOC of the battery. When the SOC of the battery is near the upper or lower limits, the BMS limits the battery-charging current, which forces the controller to decrease the regenerative torque and increase the mechanical friction braking.

4.9 Brake Force Distribution

4.9.1 Brake Force Distribution Strategy

The objective of brake force distribution is to achieve the required vehicle deceleration while maintaining longitudinal stability and preventing wheel lock-up, particularly at the rear axle. In a regenerative braking system, this objective must be satisfied while maximizing energy recovery within tire, motor, and battery limits.

Static Axle Load and Brake Force Distribution

Under static conditions, the total braking force F_{tot} is distributed between the front and rear axles according to the vehicle geometry:

$$F_{front,static} = F_{tot}\frac{L_r}{L}$$

$$F_{rear,static} = F_{tot}\frac{L_F}{L}$$

Dynamic limits override static distribution to maintain stability and prevent rear lock-up.

Dynamic Load Transfer during Braking

During deceleration, longitudinal load transfer occurs from the rear axle to the front axle. The magnitude of load transfer given by:

Brake force distribution must satisfy vehicle stability under dynamic load transfer while maximizing front-axle regenerative braking. During deceleration, load shifts forward by:

$$\Delta W = \frac{h \times m \times a}{L}$$

This load transfer increases the normal force on the front axle and reduces it on the rear axle.

Dynamic Tire–Road Friction Limits

Considering tire road friction, the maximum allowable braking forces at each axle become:

$$F_{front} \leq \mu\,(Wf_0 + \Delta W)$$

$$F_{rear} \leq \mu\,(W r_0 - \Delta W)$$

These dynamic limits override the static brake force distribution and are critical to prevent rear wheel lock-up, which would compromise vehicle stability.

4.9.2 Regenerative and Mechanical Braking Allocation

Based on the above constraints, the braking strategy adopted in this study is as follows:

Front axle: - Regenerative braking prioritized on the front axle, operating up to the minimum of motor torque limits, battery charging limits, and front axle tire–road friction limits.

Supplementary front mechanical braking

Mechanical braking added at the front axle only when regenerative braking alone is insufficient to meet the total required braking force.

$$F_{front} = F_{regen} + F_{mech,front}$$

Rear axle: - Braking provided exclusively by mechanical friction brakes to ensure stability, as regenerative braking at the rear axle under reduced normal load increases the risk of wheel slip.

$$F_{rear} = F_{mech,rear}$$

4.9.3 Total Required Braking Force and regenerative braking energy

The total longitudinal braking force required to decelerate the vehicle given by:

$$F_{tot} = \mathrm{m} \times \mathrm{areq}$$

For a moderate braking scenario representative of urban driving, a target deceleration of:

$$areq = 0.3g = 0.3 \times 9.81 = 2.94 \mathrm{m/s^2}$$

$$F_{tot} = 950 \times 2.94 = 2793\,N$$

This is the total braking force that must be generated by the combination of regenerative and mechanical braking.

Kinetic Energy at 50 km/h, Initial speed = 13.88m/s

$$E_K = \frac{1}{2} m\,V^2$$

$$= \frac{1}{2}(950)\ 13.88^2$$

= 91,611.7 J

Converting joules to watt-hours for comparison with electrical energy

$$E_K = \frac{91{,}611.7\ \text{J}}{3600} \quad = 25.45\ Wh$$

Relation to Regenerative Braking

From Section 4.7, the available regenerative braking force was calculated as:

$$F_{regen,total} = 5084\ N$$

$$F_{regen,total} > F_{tot}$$

The regenerative braking system is capable of supplying the entire required braking force for this moderate deceleration without assistance from mechanical brakes, subject to battery and SOC limitations discussed in Section 4.8.

In practice, only a fraction of the kinetic energy can be recovered due to electrical, mechanical, and battery efficiency losses, as well as control constraints

4.9.4 Battery-Limited Regenerative braking Power

Although the motor is capable of generating higher regenerative torque, the battery charging current imposed by the Battery Management System (BMS) limits the maximum usable regenerative power.

The allowable battery charging power is taken from section 4.8:

$$P_{batt,allowed} = 22{,}500W$$

Considering drive train to battery efficiency η=0.85, the corresponding mechanical regenerative power at the motor shaft is

Mechanical shaft power, $P_{regen,shaft} = \frac{P_{batt,allowed}}{\eta}$

$$= \frac{22{,}500}{0.85}$$

= 26,470 W = 26.47 kW

Maximum Regen Braking Force at 50 km/h

The braking force associated with this power at vehicle speed v is obtained from:

$$F_{regen,max} = \frac{P_{regen,shaft}}{\mathrm{V}}$$

$$= \frac{26{,}470}{13.89}$$

= 1,905.7 N

This represents the maximum braking force that can be supplied by regenerative braking at 50 km/h under battery current limitations.

4.9.5 Static Brake Force Distribution

Static front share:

$$F_{front,static} = F_{tot}\frac{L_r}{\mathrm{L}}$$

$$= F_{tot}\frac{1.2}{2.2}$$

$$= 0.545\, F_{tot}$$

Static rear share:

$$F_{rear,static} = F_{tot}\frac{L_f}{\mathrm{L}}$$

$$= F_{tot}\frac{1.2}{2.2}$$

$$= 0.455\, F_{tot}$$

4.9.6 Mechanical Braking Requirement

For the selected deceleration: $areq = 3\mathrm{m/s^2}$

$$F_{tot} = \mathrm{m} \times \mathrm{areq}$$

$$= 950 \times 3$$

$$= 2850\ \mathrm{N}$$

Mechanical brakes must provide the remaining braking force:

$$F_{mech,needed} = F_{tot} - F_{regen,max}$$

Calculated Max regen = 1695 N $F_{mech,needed} = 2850 - 1695$

$$=1155\ \mathrm{N}$$

The regenerative braking system cannot supply the full-required braking force due to battery power limitations then Mechanical front braking added.

Fraction of braking provided by regeneration

The fraction of braking provided by regenerative braking is:

$$Regen\ fraction\ = \frac{1695}{2850}\ =\ 0.595$$

Regen fraction=59.5% and Mechanical fraction=40.5%

Assuming that braking force contribution is approximately proportional to energy dissipation during a moderate braking event, the energy recovered through regenerative braking is:

$$E_{regen} = 0.595 \times 25.45$$

$$= 15.1Wh$$

The remaining energy: $E_{mech} = 25.45 - 15.1$

$$= 10.35\,Wh$$

10.35 wh is dissipated through mechanical braking.

4.9.7 Energy recovered and system efficiency for this stop

$$\eta_{system} = \frac{E_{regen}}{E_k} \times 100\%$$

$$\eta_{system} = \frac{15.1\ Wh}{25.45\ \text{Wh}} \times 100\%$$

$$= 59.5\%$$

This result shows that for a moderate deceleration of 3 m/s² at 50 km/h, the regenerative braking system supplies approximately 60% of the total braking energy, with mechanical brakes providing the remaining 40% to satisfy battery and power constraints.

Regenerative Braking Performance at gentle (2 m/s²) Deceleration (gentle / comfort braking)

The following table presents the kinetic energy of the vehicle at different speeds and the recoverable energy through regenerative braking within the constraints of the designed vehicle's regenerative braking system. Regenerative braking is restricted by the maximum current supplied by the BMS (80 A), battery voltage (250 V), and efficiency of the motor and dc-dc converter combination ((η = 0.85).

The deceleration required is fixed at 2 m/s², and therefore the total required braking force is 1,900 N. For lower speeds, regenerative braking can provide all the required braking force, but at higher speeds, the regenerative braking force will be lower than the required force, and therefore mechanical braking will have to be applied in order to attain the required deceleration.

Table 4. 9: kinetic and regenerative force at various speed at 2 m/s² deceleration

Speed (km/h)	$E\_k\ (Wh)$	$E\_regen\ (Wh)$	$\eta_{system}(\%)$
10	1.02	0.87	85
20	4.08	3.47	85
30	9.18	7.80	85
40	16.33	13.88	85
50	25.45	22.60	75.8
60	36.65	27.23	74
70	49.85	31.74	64
80	65.06	36.31	56
90	82.30	40.75	49
100	101.56	45.29	45

From the table, it is clear that the regenerative braking system can recover all kinetic energy at low speeds (≤40 km/h). At higher speeds, the system efficiency decreases because the maximum regenerative braking force limited by the motor, bms and battery constraints. This highlights that while the regenerative system significantly reduces reliance on mechanical braking, mechanical brakes at moderate to high speeds to maintain the requested deceleration of 2 m /s² must still handle a portion of the braking energy.

Regenerative Braking Performance at gentle (3 m/s²) Deceleration (typical urban braking)

The tables below show how much of the vehicle's kinetic energy can be recovered by regenerative braking when the vehicle is slowed by two different rates of deceleration, 3 m/s² and 6 m/s². The regenerative braking force is limited by the battery, 20 kW electric, 23.5 kW mechanical, η = 0.85, so the efficiency of regenerative braking drops rapidly as the vehicle's speed increases, because more braking force is required for higher rates of deceleration, resulting in less regenerative braking force, therefore less efficient energy recovery.

Table 4. 10: kinetic and regenerative force at various speed at 3 m/s² deceleration

Speed (km/h)	**v (m/s)**	E_k (Wh)	**Regen Fraction**	E_regen (Wh)	**η system (%)**
10	2.78	1.02	1.00	0.87	85
20	5.56	4.08	1.00	3.47	85
30	8.33	9.16	1.00	7.79	85
40	11.11	16.29	0.95	13.12	80.5
50	13.89	25.47	0.91	19.6	77
60	16.67	36.68	0.84	26.1	71
70	19.44	49.88	0.75	31.8	64
80	22.22	65.18	0.67	36.9	57
90	25.00	82.47	0.61	42.7	52
100	27.78	101.97	0.55	47.5	46.6

Regenerative Braking Performance at moderate (6 m/s²) Deceleration (aggressive-emergency braking)

The tables below indicate how much of the vehicle's kinetic energy can be recovered using regenerative braking at two deceleration levels (6 m/s²). Regenerative braking force is limited by the battery's capability, 25 kW electrical and 23.5 kW mechanical at η = 0.85. As speed increases, efficiency drops sharply because higher deceleration requires higher braking force and therefore lower regenerative braking force, thus lower energy recovery efficiency.

Table 4. 11: kinetic and regenerative force at various speed at 6 m/s² deceleration

Speed (km/h)	**V(m/s)**	$E_K(wh)$	$E_{regen}(kw)$	η_{system} (%)
10	2.78	1.02	1.02	-
20	5.56	4.08	2.74	67.0
30	8.33	9.16	4.12	45.0
40	11.11	16.29	5.54	34.0
50	13.89	25.45	6.87	27.0
60	16.67	36.68	8.07	22.0
70	19.44	49.88	9.48	19.0
80	22.22	65.18	11.08	17.0
90	25.00	82.47	12.37	15.0
100	27.78	101.97	13.26	13.0

For high levels of deceleration (6 m/s²), the total braking force demand far exceeds the battery-limited regenerative braking capability. With increasing vehicle speed, the maximum regenerative force available decreases proportionally to the inverse of the vehicle speed, resulting in a sharp decrease in the amount of recoverable energy. In this case, mechanical brakes dominate the vehicle, especially at medium and high speeds, resulting in less than 30% overall energy recovery efficiency when the vehicle speed is more than 50 km/h.

4.10 Instantaneous Regenerative Power Limited by Vehicle Dynamics and Battery Constraints

Step a power demanded by vehicle dynamics (theoretical maximum recoverable power):

Dynamic braking power available from vehicle motion at 50 m/s given by

$$P_{dyn} = \text{m} \times \text{a} \times \text{v}$$

$$=950\times2\times13 = 26{,}361 \text{ W}$$

Mechanical power at motor shaft during regeneration

$$P_{motor,regen} = P_{dyn} \times \eta_{total}$$

$$= 26361 \times 0.765 = 20{,}165 \text{ W}$$

Actual battery charging power: Battery only receives a part of motor shaft power:

Table 4. 12: battery charging energy limitation during instant regenerative braking

Speed (km/h)	**Velocity (m/s)**	$\boldsymbol{P_{dyn}(W)}$	$\boldsymbol{P_{motor,regen}}$**(w)**	$\boldsymbol{P_{batt}}$**(W)**	**Limit Applied (W)**
10	2.78	5,277	4,486	3,813	3,813
20	5.56	10,555	8,972	7,626	7,626
30	8.33	15,833	13,458	11,439	11,439
40	11.11	21,111	17,944	15,252	15,252
50	13.89	26,388	22,430	19,065	19,065
60	16.67	31,666	26,916	22,879	Limited
70	19.44	36,944	Limited	26,692	Limited
80	22.22	42,222	Limited	30,505	Limited
90	25.00	47,500	Limited	34,318	Limited
100	27.78	52,777	Limited	38,131	Limited

At low to moderate speeds, the regenerative braking system works below the battery's charging power limit, enabling almost the entire dynamically available braking power to be converted to electricity.

At speeds higher than 50 km/h, the dominant limit becomes the battery's charging power limit, which is 20 kW. Although the motor has the ability to recover more power, the battery lacks the ability to accept more, which leads to a decline in the regenerative braking efficiency at higher speeds, implying that more of the braking energy has to be dissipated mechanically.

4.11 Thermal Analysis

This calculation considers motor losses only; inverter thermal losses are treated separately or assumed dissipated via the inverter cooling system.

4.11.1 Power loss calculation

- $P_{loss} = P_{shaft}\,(1 - \eta_{motor}),\quad \eta_{motor}$ =0.9

$$= 0.10 P_{shaft}$$

$P_{shaft} = P_{motor,regen}$ =22,430W

At 50km/h Heat accumulated in a 10-second braking event

$$P_{loss} = 0.10 \times 22{,}430.6$$

$$= 2{,}243W$$

$$E_{heat} = P_{loss} \times t$$

$$= 2{,}243W \times 10s$$

$$= 22{,}430J,$$

A lumped motor thermal capacitance of 6 kJ/K is assumed, consistent with reported values for compact EV traction motors.

$$\Delta T = \frac{E_{heat}}{C_{thermal}}$$

$$=\frac{22.4\text{kj}}{6\text{ kj/k}}$$

$$= 3.7°\text{C}$$

A single strong 10-second regenerative event raises motor temperature by 3.7°C — completely safe.

However, multiple back-to-back high-speed regen events will accumulate heat, and temperature can climb rapidly if airflow is poor. However, repeated high-power regenerative events with insufficient cooling time will cause cumulative temperature rise, potentially pushing the motor toward its thermal limit under sustained urban or downhill driving conditions.

4.12 Controller calculation

1. Torque Control and Saturation

- The controller limits the torque to avoid exceeding motor or battery limits.
- Include:
    - Torque demand including inertia

$$T_{demand,total} = T_{driver} + J_{drivetrain} \times \alpha$$

Linear deceleration to angular acceleration at given a=−5.0 m/s²

$$\alpha = \frac{a}{r_w}$$

$$= \frac{-5}{0.29} \quad =17.24 \text{ rad/s}^2$$

Braking force, $F = ma$

$$= 950 \times (5)$$

$$= 4750\ N$$

Wheel torque from braking force, $T_{driver} = F_{brake} \times r_w$

$$T_{driver} = 4750 \times 0.29$$

$$=1377.5\ \text{Nm}$$

Inertia torque, $T_{inertia} = J_{drivetrain} \times \alpha$

$$T_{inertia} = 10 \times 17.24$$

$$= -172.4\ Nm$$

$$T_{demand,total} = T_{driver} + J_{drivetrain} \times \alpha$$

$$= 1377.5\ Nm + (172.4\ N)$$

$$= 1549.9Nm$$

This is the mechanical torque at the wheel required to achieve the desired deceleration of –5 m/s², including both braking force and drive train rotational inertia.

Convert Wheel Torque to Motor Shaft Torque

$$T_{motor} = \frac{T_{wheel}}{\text{ig} \times \eta_{\text{td}}}$$

$$= \frac{1549.9}{13 \times 0.9}$$

$$=132.5\text{Nm}$$

The gearbox reduces torque by the gear ratio. After accounting for 85% efficiency, the motor must supply about 132.5 of regenerative torque to achieve –5 m/s² braking.

This is the torque the controller, must command for regen at –5 m/s².

Torque saturation (limit check):
Max allowable torque:

$$T_{max} = (I_{max}) \times k_t$$

$$= 0.425 \times 180$$

$$= 76.2 \text{N.m}$$

$$T_{wheel,regen} = 76.2 \times 13/0.85$$

$$= 1170 \text{ N}$$

The controller must saturate the torque at 76 NM because the battery cannot accept more than 180 A. This electrical limit is the main bottleneck not the mechanical limit.

Braking force from regenerative:

$$F = \frac{1170}{0.29}$$

$$= 4035 \text{ N}$$

This is the maximum braking force regen can generate under the BMS limited torque.

Deceleration from regen alone:

$$a = \frac{F}{m}$$

$$= \frac{4035}{950} = 4.24 \text{m/s}^2$$

Regen alone provides about 4.24 m/s² deceleration, which is good for mild braking but not enough for braking (5 m/s²). In this case Mechanical brakes must handle the remaining 0.7 m/s².

2. Motor Current and Voltage Relations

- PWM control and duty cycle equations:

$$V_{avg} = D \times V_{batt}$$

$$=0.8\times250$$

$$= 200\text{V}.$$

$$E_{back} = K_e \times \omega_m, \quad \omega_m = \frac{E_{back}}{Ke}$$

$$= \frac{274}{0.425}$$

$$=644\text{rad/s at 50 km/h}$$

$$T_{motor} = K_t \times \text{I}, \quad \text{I} = 0.425 \times 180$$

$$= 76.5nm$$

3.Maximum regen current limited by SOC and BMS:

Power flow balance:

$$P_{regen} = T_{regen} \times \omega_m$$

$$= 76.4 \times 644$$

$$= 49.2\ KW$$

Power to battery: $P_{batt} = P_{regen} \times \eta_{motor} \times \eta_c$

$= 49{,}206 \times 0.9 \times 0.95$

$= 42\text{kw}$

Battery current: $I_{batt,motor} = \frac{P_{batt,motor}}{V_{batt}}$

$= \frac{42\ kw}{250}$

$=168\ \text{A}$

SOC Variation During a Braking Event

SOC change during 10s braking

$$\Delta\text{SOC} = \int_{t0}^{t1} \frac{I_{batt}}{C_{batt}}\ \text{dt}$$

$$\Delta\text{SOC} = \int_{0}^{10} \frac{I_{batt}}{C_{batt}}\ \text{dt}$$

$\Delta\text{SOC axle} = \frac{t}{3600}$, t=10s

$=\frac{168.2\times10}{100\times3600}$

$=0.0467$

4. Field Weakening and Speed Control

Motor Current for Torque (I_q)

$I_q = \frac{T}{K_t}$

$= \frac{27.28}{0.425}$

=64.2A

ω=v×45.5

@ low speed Case 1: v=−2.0 m/s

ω_1 =−2.0×45.5=−91 rad/s

$$I_d = \frac{-V_{limit} - (K_e \omega)}{L_d \omega}$$

$$I_d = \frac{-250 - (0.425 \times (-91))}{0.002 \times (-91)}$$

=1161A

Field weakening is not applied at low speed the controller just ignores I_d here because you're nowhere near voltage limit.

@ High-speed Case 2: v=−5.0 m/s

ω_2=−5.0×45.5=−227.9 rad/s

$$Id = \frac{-V_{limit} - Ke\omega}{L_d \omega}$$

$$Id = \frac{-250-(0.425\times(-227))}{0.002\times(-227)}$$

=337A

Suppose it's ω_{base}= 600 rad/s from earlier 50 km/h motor speed

Check if ω>ω_{base} then apply weakening logic.

So in this design**,** field weakening only becomes relevant at much higher speeds

Fuzzy controller design

A block diagram of the system consisting of a fuzzy controller. The specific design process of fuzzy controller is as follows:

1) Determine the input language variables for error e and error change ec, the output variable is r.

2) select fuzzy

3) Determine fuzzy control rules.

4) By resolving the ambiguity, the output control R, and then after processing, the output voltage.

Design of fuzzy logic

In the Fuzzy Logic Controller (FLC), the input and output variables have been defined using custom triangular membership functions to represent the various ranges of the system's behavior. For this problem, the Mamdani-type FLC provided in the MATLAB/Simulink tool is used, which is effective for handling non-linear and uncertain systems. The developed fuzzy model is depicted in the following figure.

Fuzzy rules are defined based on the control objectives and system requirements to be achieved. For this problem, the FLC is developed to control and optimize the braking force distribution between the front and rear wheels of the vehicle, ensuring smooth, stable, and efficient braking operations. The braking force distribution is affected by various parameters, including the applied braking force, state of charge of the battery, and vehicle speed. By dynamically adapting the braking torque based on the inputs, the FLC improves the overall safety and regenerative energy harvesting during the braking maneuvers of the vehicle.

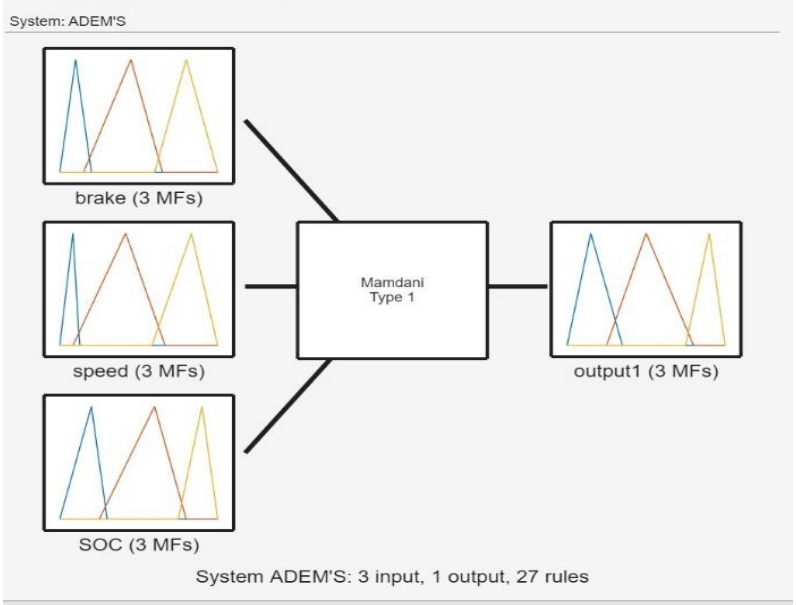

Figure 4. 4: Mamdani-type fuzzy inference system architecture for regenerative braking control, showing input variables and output command

A. brake

The relationship between the driver's braking demand and vehicle safety can be related to the fact that the vehicle's braking force has a direct effect on the vehicle's stopping distance and reaction time. A high braking force is likely to be a sign that the vehicle is in an emergency stop situation that requires immediate attention, and hence the amount of regenerative braking force should be minimized to maximize the mechanical braking force. However, when the vehicle is in a moderate braking situation, the amount of regenerative braking force can be maximized to achieve the desired results. For light braking, the amount of regenerative braking force can be maximized to achieve the desired results.

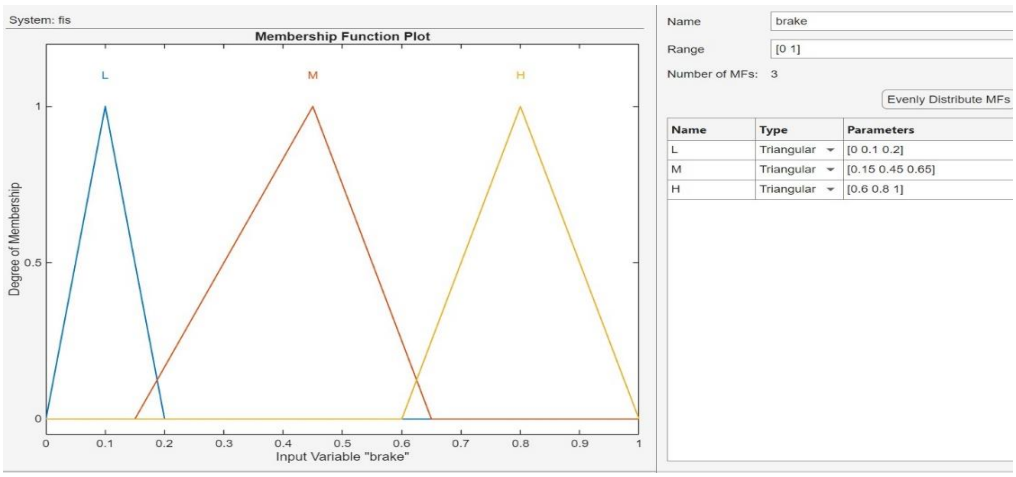

Figure 4. 5: Membership functions of brake pedal demand used as a fuzzy input to represent driver braking intention

B. The state of charge (SOC)

SOC of the battery also plays a crucial role in determining the amount of regenerative braking force that can be used. If the SOC is less than 10%, the internal resistance of the battery will be high, and it will not be desirable to charge the battery. In this case, the regenerative braking force should be minimal. If the SOC is in the range of 10 to 90%, the battery can be charged, and hence the regenerative braking force can be maximized. However, if the SOC is more than 90%, the charging current should be reduced to prevent lithium-ion plating, and hence the regenerative braking force should be reduced.

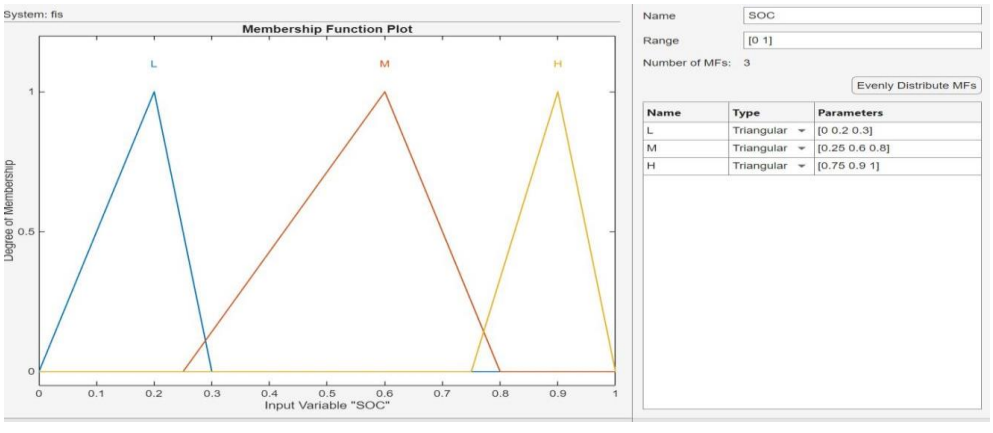

Figure 4. 6: Membership functions of battery state-of-charge (SOC) employed as a fuzzy input to regulate regenerative braking intensity

C. SPEED

Another significant factor that affects vehicle speed and braking safety and energy recovery is vehicle speed itself. When the vehicle speed is low, it is important that regenerative braking torque is kept at a minimum level. As the vehicle speed rises and becomes moderate, regenerative braking may be increased to an appropriate level. When the vehicle speed rises and becomes higher, regenerative braking force may be increased to a maximum level.

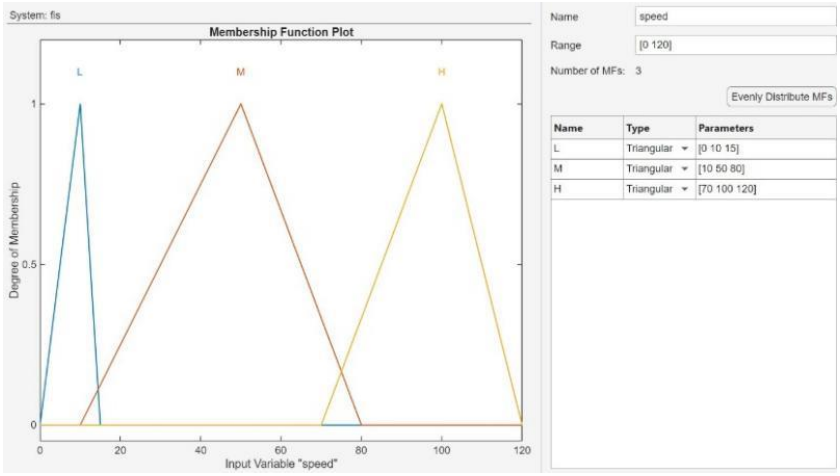

Figure 4. 7: Membership functions of vehicle speed used as a fuzzy input variable in the regenerative braking controller

Based on these considerations, three input variables are defined for the fuzzy logic controller (FLC): braking force, state of charge (SOC), and vehicle speed. The membership function for braking force is represented by three linguistic variables—Low, Medium, and High.

Rules of fuzzy logic

- The fuzzy rules set in the controller's rule base is 27 in number, as depicted in Figure 4.8. These rules describe the logical relationship between the three input variables: the braking force, the speed of the vehicle, and the state of charge (SOC), and the single output variable, which is

the output related to the regenerative braking (output r). Each of the rules is of the IF-THEN type, which is common in Mamdani-type fuzzy logic controllers.

These three input variables have each been partitioned into three levels:

- Braking force: Low (L,), Medium (M,), High (H)
  - Vehicle speed: below 15KM/h Low (L), between (15-80 KM/h) Medium (M), above 80KM/h High (H)
  - State of charge (SOC): Low (L), Medium (M), High (H)

The combination of these linguistic variables results in a total of 3×3×3=27 possible conditions, which form the complete rule base. Each rule determines the corresponding output level Low, Medium, or High of the regenerative braking effort.

System: ADEM'S

Add All Possible Rules | Clear All Rules

	Rule	Weight	Name
1	If brake is L and speed is L and SOC is L then output1 is L	1	rule1
2	If brake is M and speed is L and SOC is L then output1 is L	1	rule2
3	If brake is H and speed is L and SOC is L then output1 is L	1	rule3
4	If brake is L and speed is M and SOC is L then output1 is H	1	rule4
5	If brake is M and speed is M and SOC is L then output1 is H	1	rule5
6	If brake is H and speed is M and SOC is L then output1 is M	1	rule6
7	If brake is L and speed is H and SOC is L then output1 is L	1	rule7
8	If brake is M and speed is H and SOC is L then output1 is H	1	rule8
9	If brake is H and speed is H and SOC is L then output1 is M	1	rule9
10	If brake is L and speed is L and SOC is M then output1 is L	1	rule10
11	If brake is M and speed is L and SOC is M then output1 is L	1	rule11
12	If brake is H and speed is L and SOC is M then output1 is L	1	rule12
13	If brake is L and speed is M and SOC is M then output1 is H	1	rule13
14	If brake is M and speed is M and SOC is M then output1 is H	1	rule14
15	If brake is H and speed is M and SOC is M then output1 is M	1	rule15
16	If brake is L and speed is H and SOC is M then output1 is H	1	rule16
17	If brake is M and speed is H and SOC is M then output1 is M	1	rule17
18	If brake is H and speed is H and SOC is M then output1 is M	1	rule18
19	If brake is L and speed is L and SOC is H then output1 is L	1	rule19
20	If brake is M and speed is L and SOC is H then output1 is L	1	rule20
21	If brake is H and speed is L and SOC is H then output1 is L	1	rule21
22	If brake is L and speed is M and SOC is H then output1 is L	1	rule22
23	If brake is M and speed is M and SOC is H then output1 is L	1	rule23
24	If brake is H and speed is M and SOC is H then output1 is L	1	rule24
25	If brake is L and speed is H and SOC is H then output1 is L	1	rule25
26	If brake is M and speed is H and SOC is H then output1 is M	1	rule26
27	If brake is H and speed is H and SOC is H then output1 is H	1	rule27

Figure 4. 8: Fuzzy rule base consisting of 27 control rules defining the relationship between inputs to determine the regenerative braking output

The logic of these rules is designed in such a manner that it facilitates smooth braking characteristics, safety, and maximum energy recovery:

If the braking force and speed are low or if SOC is at its limits (very low or very high), then the output will be Low, indicating that there will be minimum regenerative braking to protect the battery and provide a comfortable ride. For average braking conditions, medium speeds, and average SOC levels, the output will normally be Medium, enabling efficient regenerative braking. In cases of high braking force and vehicle speed, if SOC levels are within an acceptable range, then the output will be High, enabling maximum regenerative braking.

All of these rules are given equal weightage, and each rule will contribute equally in the final decision-making process of the fuzzy inference system.

Defuzzification

The centroid method, also known as the center of gravity method, is widely used for defuzzification in fuzzy logic controllers. It determines the crisp output value by calculating the weighted average of the output variable over the aggregated membership function. This method provides a smooth and balanced control response, making it suitable for applications such as regenerative braking systems where gradual and stable control action is required.

The last step in the Fuzzy Logic Controller (FLC) is Defuzzification, in which the fuzzy output values from the inference engine are converted into a crisp output value that can be used to operate the system, such as the motor or the brakes.

The formula for centroid method is given by

Centroid Method $y = \frac{\int y\mu(y)dy}{\int \mu(y)dy}$

$$y = \frac{\sum yi\mu(yi)}{\sum \mu(yi)}$$

5. Brake System Integration

When integrating the regenerative braking (RB) system into the existing vehicle, it is important to note the interaction between the RB system and the existing braking systems. For the 1987 Toyota Corolla, the following considerations are important when integrating the RB system:

a. Retention of Original Hydraulic Brake System

The original hydraulic braking system is retained for reliability and safety purposes. The RB system should work in harmony with the existing braking systems without compromising the braking performance of the vehicle. This provides redundancy for the vehicle, such that if the regenerative braking is not effective (e.g., during low vehicle speeds), the vehicle can still come to a complete stop using the hydraulic brakes.

b. Brake Pedal Sensor / Position Encoder

A brake pedal sensor is required to measure the driver's braking intent accurately. This signal enables the RB system to modulate regenerative torque in proportion to pedal input, ensuring a smooth and predictable deceleration. Both displacement-based and force-based sensors can be employed, providing the control system with real-time information for brake blending or additive braking scenarios. Accurate sensing is crucial for driver perception and safety, especially during emergency braking or sudden pedal inputs.

c. Brake Torque Split and Control Strategy

For effective regenerative braking to occur, the braking torque should be distributed effectively between the electric motor and the friction brakes. The two main methods for achieving this include: Additive braking: The regenerative torque is added to the hydraulic braking torque. Using this method ensures ease of integration without requiring changes to the existing brake systems. and The control strategy should also include consideration of vehicle speed, wheel slip, and battery state-of-charge to prevent instabilities. For instance, during high regenerative braking, the torque can be reduced at the rear wheels to prevent lock-up.

d. Safety and Redundancy

Safety is of prime importance in the integration of the regenerative braking system. The regenerative braking system must be designed to be fail-safe, such that if the regenerative braking system fails, the hydraulic braking system will be available to provide maximum braking capacity to the vehicle. In case of panic braking or sudden braking, the regenerative braking must be designed to ramp down smoothly to prevent any sudden behavior of the vehicle.

e. Vehicle-Specific Integration Considerations

In the case of the front-wheel-driven Corolla, the motor and transmission are mounted at the front axle. Therefore, the regenerative brakes are active on the front wheels, and the controller has to consider the longitudinal load transfer during deceleration. It may also use coast regen, which is the application of mild regenerative torque when the pedal is zero to capture energy without compromising comfort and stability.

f. Control Signals and Sensor Integration

The system uses various sensor signals, such as: Wheel speed sensors for detecting slips, Brake pedal travel or force sensors, Vehicle acceleration sensors and Road friction estimation. In order to coordinate all these components properly and deliver reliable and efficient braking performance, it is necessary to coordinate the electric motor, converter, battery management system, and existing brake master cylinder.

CHAPTER FIVE

5. RESULT AND DISCUSSION

5.1 comparative result for PID and fuzzy logic controller

The comparative simulations showed the PID controller (yellow) had considerable problems in controlling the tunning process and was less stable. However, the fuzzy logic controller (red) was able to track the input signal smoothly and was very precise in tracking the reference signal with minimal overshoot and faster settling times. The above results also justify the use of the fuzzy logic controller for the main regenerative braking control due to the higher reliability in controlling the torque and the ability to handle the nonlinearity of the vehicle dynamics.

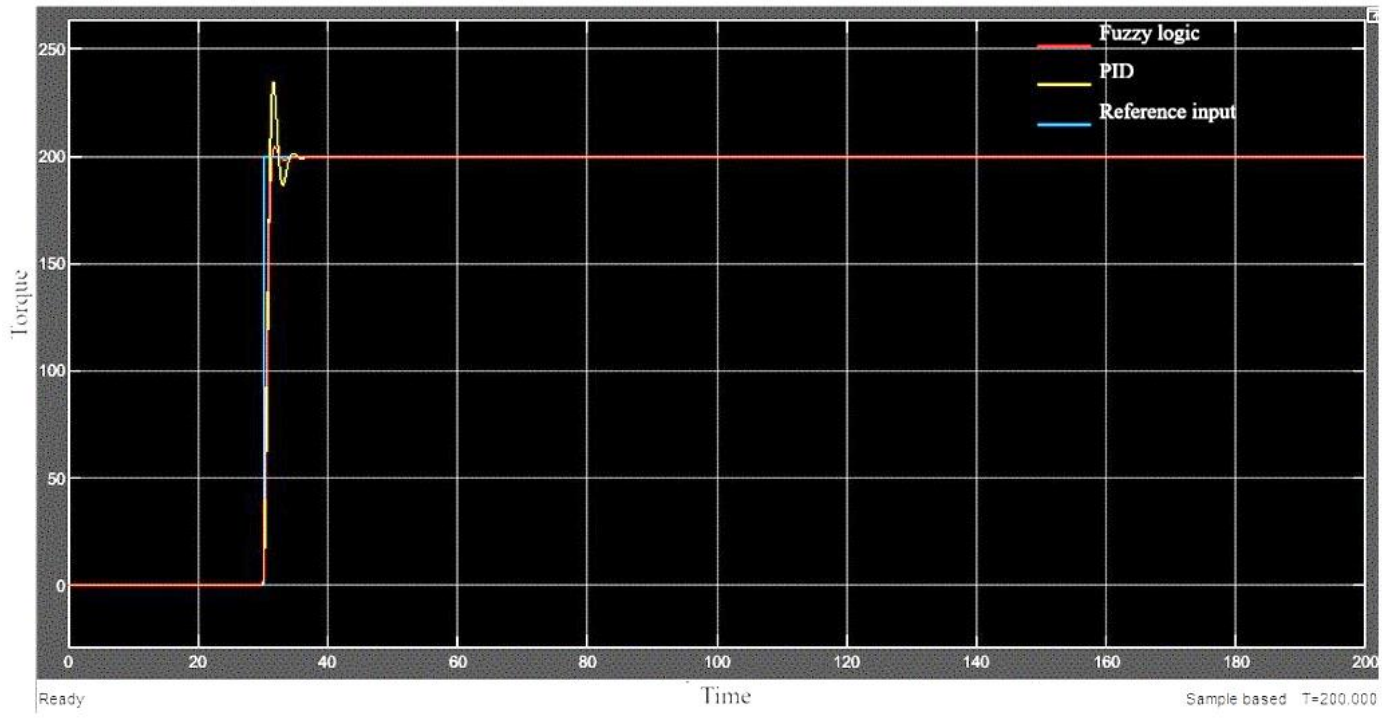

Figure 5. 1 result in tunning performance comparison between PID and Fuzzy logic control

The results showed that the PID controller has problems with tuning the controller to manage the nonlinear battery charging limitations and sudden changes in vehicle speeds. However, the FLC controller showed better performance and closer conformity to the desired braking torque profile.

Therefore, the FLC controller was selected for integration with the final system due to its robust performance in the nonlinear operating conditions expected in regenerative braking systems.

5.2 Regenerative Braking Functional Validation Using Torque Step Input

However, before the evaluation of the system under the standardized drive cycle, a preliminary functional validation of the regenerative braking capability was performed by the application of a step torque input signal. This was done as an additional test case, aimed at isolating the bidirectional energy flow characteristic of the electric drive train, avoiding the added complexity of the longitudinal vehicle motion and the various speed profiles.

The step torque was applied to the motor shaft, with the step time being 7 seconds, going from an initial braking torque of -20 Nm to a driving torque of +10 Nm, with the negative region corresponding to the regenerative braking mode and the positive region corresponding to the traction mode.

The State of Charge response of the battery as a result is depicted as shown in the Figure below. From the above figure, it is noted that during the period of time between 0s and 7s, when a negative torque is applied, the SOC of the battery gradually increases. This is an indication that energy is being supplied back into the battery pack. This is a confirmation that the machine is indeed in generator mode.

At t = 7s, the torque changes its value from negative to positive. This is an indication that the machine is now in propulsion mode. At this time, the SOC starts reducing as energy is drawn from the battery pack. The clear change in SOC trend at the torque reversal point demonstrates correct directional energy flow control within the system.

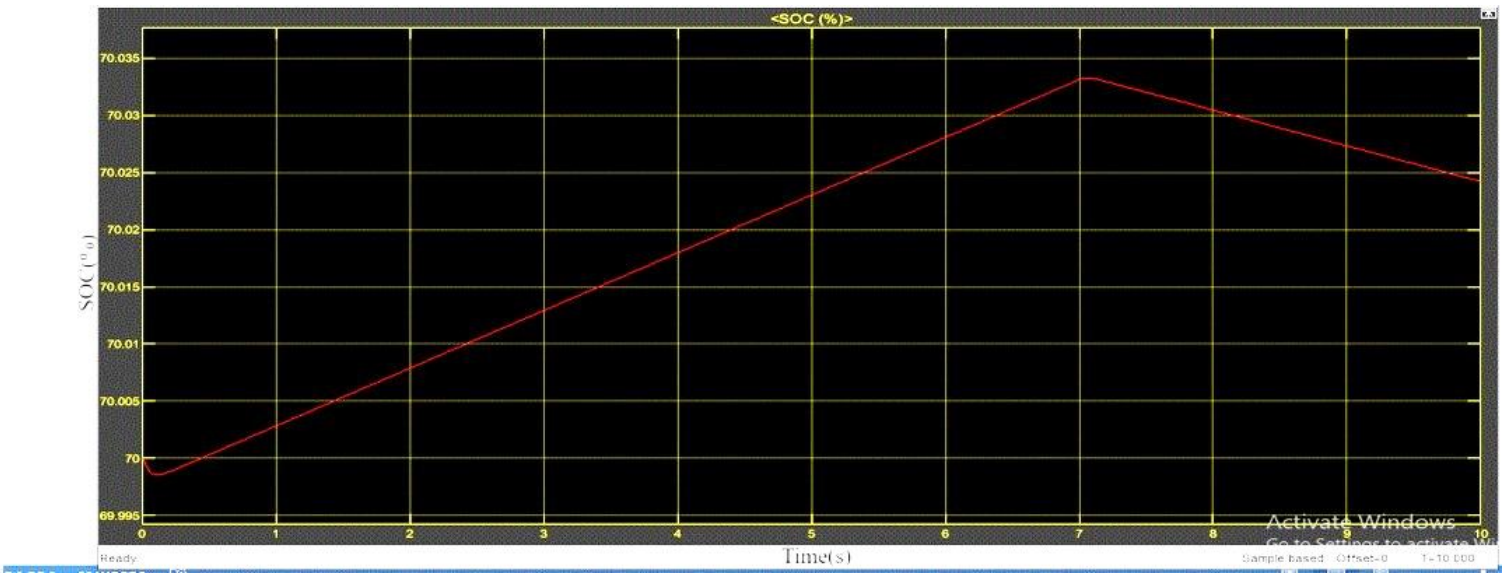

Figure 5. 2: result in highlighting energy recovery during stop-and-go events

The torque step test verifies that the regenerative braking system functions correctly. The increase in battery SOC after the negative torque time interval from 0 to 7 seconds indicates that regenerative braking and battery charging are working correctly and that generator-mode operation of the electrical machine is verified. The decrease in SOC after the torque transition from negative to positive indicates correct battery discharge and traction operation.

Although it does not simulate real-world driving scenarios, it is an effective test in verifying bidirectional power flow and control logic, as seen in various regenerative braking studies.
It was verified that the system was operating correctly and was ready for further testing under standardized drive cycle conditions.

5.3 FTP-75 Drive Cycle Results with and Without Regenerative Braking

The performance of the proposed electric vehicle model was evaluated using the FTP-75 urban drive cycle test, which is commonly used for simulating stop-and-go driving patterns common in urban driving scenarios. The FTP-75 urban drive cycle test has a total time of 2474 seconds and a total distance of 17.9354 km. As it involves a large number of acceleration and deceleration modes, it is suitable for evaluating regenerative braking systems.

To quantify the impact of regenerative braking on vehicle energy performance, two simulation scenarios were considered: Vehicle operation with regenerative braking enabled, and Vehicle operation without regenerative braking, where all braking energy is dissipated through mechanical braking.

In both cases, the battery initial State of Charge (SOC) was set to 70% to ensure a fair comparison under identical initial conditions.

The Figure below illustrates the battery SOC profiles for the scenarios over the duration of the FTP-75 cycle.

1. Vehicle Performance Without Regenerative Braking In the case without regenerative braking, the battery SOC decreases continuously throughout the drive cycle, reaching a final value of 61.79%. This behavior reflects the exclusive reliance on the battery to supply traction power, with no energy recovery during braking events. The battery state of charge (SOC) decreased by 8.21% over a driving distance of 17.954 km under the FTP-75 driving cycle. Assuming a linear relationship between SOC depletion and distance traveled, the estimated total driving range of the vehicle is approximately 218.46 km for a fully charged battery.

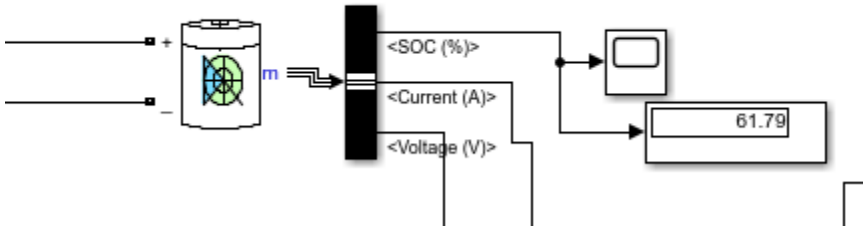

Figure 5. 3: result in Real-time battery SOC shown in Simulink during without regenerative braking operation

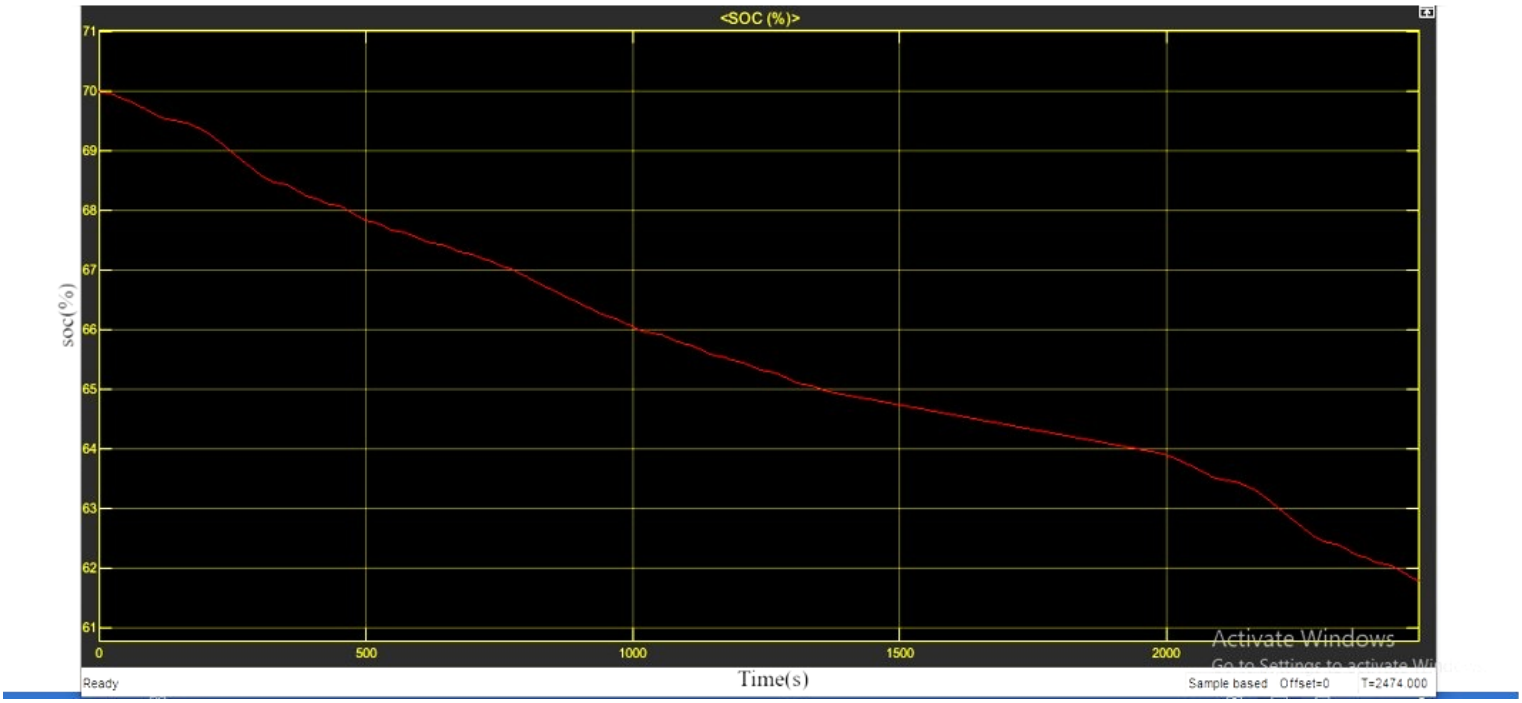

Figure 5. 4: result in Simulink display of battery SOC under FTP-75 drive cycle

The remaining soc after the it depleted in the drive cycle 61.79% from 70% initial

So, 8.21% is depleted.

8.21% = 17.954 km (total distance covered during the ftp drive cycle)

100% = x

Total Range=$(17.954 \times 100)/8.21 \approx 218.8$ km

2. Vehicle Performance With Regenerative Braking

When regenerative braking is enabled, the SOC trajectory exhibits a comparatively slower rate of depletion. At the end of the drive cycle, the remaining battery SOC is 63.04%, corresponding to a net improvement of 1.25% relative to the non-regenerative case (61.79%). This difference confirms that a portion of the kinetic energy normally lost during braking is recovered and stored in the battery.

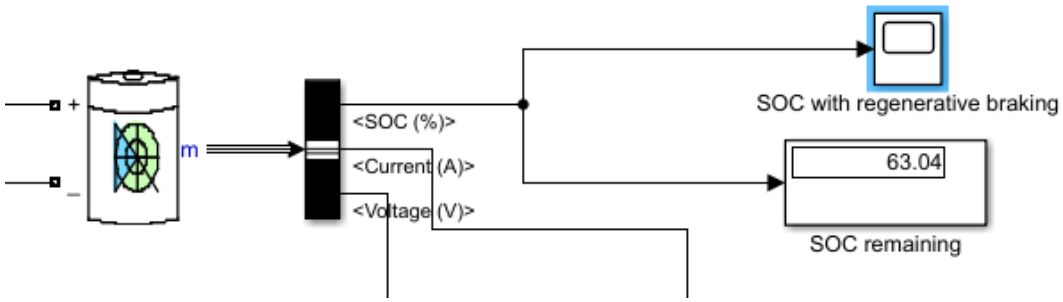

Figure 5. 5: result in Real-time battery SOC shown in Simulink during regenerative braking operation

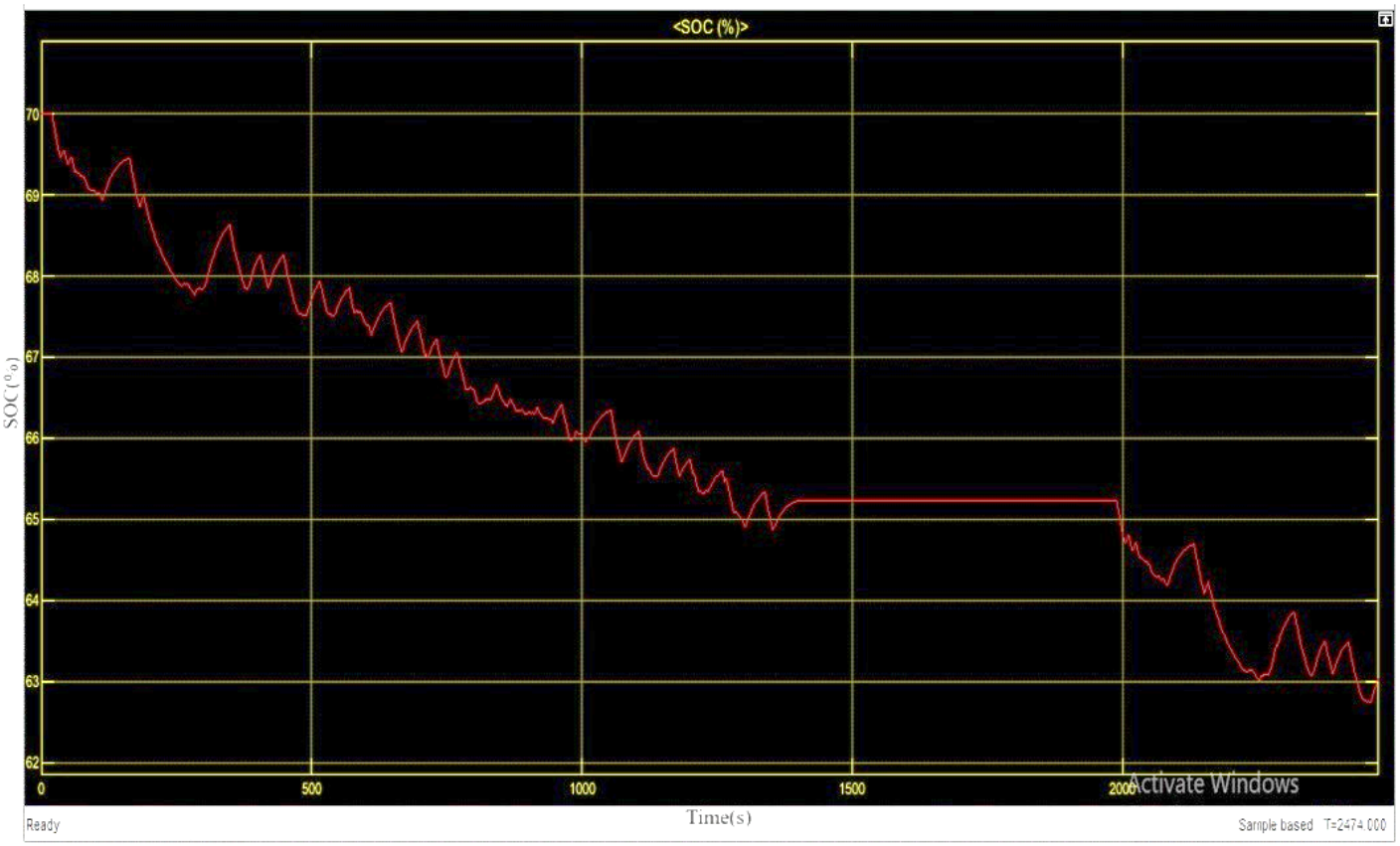

Figure 5. 6: result in Real-time battery SOC shown in Simulink during regenerative braking operation

The remaining soc after the it depleted in the drive cycle 63.05% from 70% initial

So, 6.95% is depleted.

6.95% = 17.954 km

100% = x

Range=$(17.954 \times 100)/6.95 \approx 258.3$ km

Using the total distance covered during the FTP-75 cycle and the corresponding battery energy consumption, the vehicle driving range was estimated for both scenarios. With regenerative braking enabled, the estimated driving range is 258.3 km, whereas the range without regenerative braking is 218.46 km.

So, 258.3 km-218.8 km= 39.5

This represents an increase in driving range of approximately 39.5 km, demonstrating the cumulative benefit of regenerative braking over repeated braking events within an urban driving cycle.

Estimate overall efficiency improvement

Lets calculate the increased range in efficiency

$$\eta increase = \frac{New\ range - Original\ range}{Original\ range} \times 100$$

$$\eta increase = \frac{258.3-218.8}{218.8} \times 100 \quad = 18\%$$

In addition to range enhancement, the application of regenerative braking results in an improvement in the overall system energy efficiency. Based on the ratio of useful traction energy to total battery energy consumed, the overall efficiency is observed to increase by approximately 18% when regenerative braking is incorporated.

Table 5. 1: Result Summary

Parameter	**Without RB**	**With RB**	**ENERGY RECOVERED**
Final SOC (%)	61.79	63.04	1.25%

Estimated Range (km)	218.8	258.3	39.5KM
Efficiency Improvement (%)	0	18%	18%

Comparison with existing Literature

The simulation of the proposed regenerative braking system for the small electric vehicle conversion produced an overall energy recovery efficiency of 18%. This result aligns closely with existing studies on regenerative braking in electric vehicles, demonstrating the reliability and validity of the proposed system.

For pure electric vehicles, Zhe et al. (2017) reported energy recovery efficiencies ranging from 8% to 25%, depending on vehicle configuration and driving conditions.

In terms of driving range, Nian, Peng, and Zhang (2009) observed that regenerative braking can increase EV range by 15–20%, depending on the motor and control strategy. This supports the practical significance of the 18% efficiency, indicating that even moderate energy recovery can result in meaningful extensions of driving range for small EVs.

Overall, the 18% efficiency obtained in this work is well-supported by prior studies, confirming that the proposed regenerative braking system is both feasible and effective. The results demonstrate that the system can provide measurable improvements in energy utilization and driving range, validating the thesis objective of enhancing small EV performance through regenerative braking.

DISCUSSION

As may be seen from the FTP-75 simulation results, the positive effect of regenerative braking on the overall energy performance of the converted electric vehicle is significant. Although the actual increase in the battery SOC levels at the end of the drive cycle may be low, this may be accounted for by the fact that the FTP-75 drive cycle is of short duration and that there are certain limitations on the battery charging current levels and low speed cut-off conditions that have to be taken into account.

The significant increase in the estimated range of the vehicle is a good indicator of the cumulative effect of regenerative braking under urban driving conditions, where there is a significant number of deceleration phases that allow the vehicle to regain the lost kinetic energy, resulting in a significant overall saving of battery energy levels that would have been consumed under non-regenerative conditions. This is consistent with the results reported in the existing literature on the subject, where the benefits of regenerative braking have been seen to be the most significant under low-speed conditions.

The improvement in the energy efficiency also confirms that the proposed strategy is effective in the management of the bidirectional power flow in the electric machine and the battery system. The lack of abnormal SOC variations or instability in the system during the transition in the braking process confirms that the regenerative braking system is functioning smoothly within the battery and inverter limits.

Based on the results, it can be confirmed that the regenerative braking system is effective in the management of the energy in the electric vehicle conversions, especially in the urban areas. The FTP-75 drive cycle test has confirmed the effectiveness of the proposed system in the management of the battery life, the driving distance, and the energy efficiency in the system.

CHAPTER SIX

CONCLUSION

This thesis presented the design, modeling, and simulation of a regenerative braking system for a small electric vehicle conversion. The study focused on quantifying the impact of regenerative braking on battery state of charge (SOC), energy efficiency, and driving range under urban driving conditions represented by the FTP-75 cycle.

The simulation results demonstrate that the proposed regenerative braking system effectively recovers a portion of the vehicle's braking energy, which would otherwise be dissipated as heat. This energy recovery resulted in a higher battery SOC at the end of the drive cycle, increasing from 61.79% without regenerative braking to 63.04% with it. While this increase may appear modest, it translates into a meaningful enhancement in vehicle performance, highlighting the system's practical relevance for small urban electric vehicles.

The recovered energy contributed to a range extension of approximately 39.5 km per full charge, showing that regenerative braking can significantly improve the driving capability of converted EVs. Moreover, the system achieved an overall energy efficiency improvement of 18%, confirming that the implemented fuzzy logic control strategy successfully manages bidirectional power flow with minimal losses. These results collectively indicate that regenerative braking is not merely a supplementary feature but a core performance enhancer for urban EVs, particularly those with limited battery capacity.

The study provides clear evidence that even small increments in energy recovery, when applied consistently across urban driving conditions, have a cumulative and substantial effect on vehicle operation.

In summary, this thesis establishes that regenerative braking is a practical and effective strategy for enhancing the performance of small electric vehicles. By recovering otherwise lost energy, extending driving range, and improving system efficiency, the proposed approach provides a strong technical foundation for further development of energy-optimized urban EVs.

Future work

Although the effectiveness of regenerative braking has been proven by simulation, there are areas which need to be explored to improve the efficiency of the regenerative braking system.

Firstly, the experiment could be carried out on a physical platform, which would be more convincing to prove the efficiency of the regenerative braking system.

Secondly, the regenerative braking control strategy could be made more effective by using more sophisticated control techniques such as adaptive PI control, MPC, or fuzzy control to improve the smoothness of the regenerative braking system, to recover maximum kinetic energy, and to improve the coordination of the regenerative braking system with the mechanical braking system under various conditions..

Thirdly, it is also a potential area for further research to consider the use of a combination of energy storage systems such as super capacitors and batteries. This could potentially increase the energy capture during high-power braking events.

Furthermore, it is also worth studying the effects of various drive cycles such as driving on the highway, mixed driving, and harsh driving conditions. This would enable a broader applicability of the proposed system outside the city environment for which the FTP-75 cycle is a representation.

Lastly, it is also a potential area for further research to consider the effects of battery as well as motor degradation over a series of regenerative braking events. This would enable a more comprehensive understanding of the system.

Reference

Ahmad, M. (2024). Energy recovery and control strategies for regenerative braking in electric vehicles. *International Journal of Energy Research.*

Aksjonov, A., et al. (2020). Fuzzy logic control for adaptive regenerative braking in electric vehicles. *International Journal of Vehicle Systems.*

Alam, M. (2024). Integration of supercapacitors in hybrid energy storage systems for EVs.

Barroso, J., et al. (2023). Experimental evaluation of regenerative braking systems in urban traffic. *Applied Energy, 345*, 123987.

Bian, X., & Qiu, Y. (2017). Parallel regenerative braking system design and performance analysis for electric vehicles. *Journal of Modern Transportation, 25*(2), 123–134.

Bhoopal, V., et al. (2025). Energy density and cycle life assessment of various EV battery technologies.

Brunner, P., & Brunner, R. (2021). Environmental impacts of lithium-ion vs lead-acid batteries in electric vehicles.

Chand, R., Singh, B., & Mishra, S. (2023). Impact of regenerative braking on energy efficiency and brake wear in electric vehicles. *Energy Reports.*

Chand, R., Singh, B., & Mishra, S. (2023). Performance analysis of regenerative braking systems in electric vehicles under standard drive cycles. *Energy Reports.*

Control strategy for regenerative braking based on direct torque control. (2023). *IEEE Access.*

Das, A., et al. (n.d.). Battery performance considerations in regenerative braking systems.

Dias, M., et al. (2024). Tri-mode bidirectional DC-DC converters for energy recovery applications. *Journal of Electrical Engineering.*

Doss, R., et al. (2023). BLDC motor performance for regenerative braking in EVs.

Doss, S., et al. (2023). Performance evaluation of regenerative braking using electric motors in EV applications. *Energy Reports.*

Duangtongsuk, C., et al. (2022). EV Conversion Performance Analysis and Sizing of Traction Motor and Battery from Driving Cycles. *Proceedings of ECTI-CON.* https://doi.org/10.1109/ECTI-CON54298.2022.9795372

El-Bakkouri, M., et al. (2022). Comparison of adaptive fuzzy PID and ANFIS controllers in hybrid ABS systems. *IEEE Transactions on Intelligent Vehicles.*

Esfahani, M., et al. (2024). Dynamic performance of BLDC motors in energy recovery applications.

EV Conversion Performance Analysis and Simulation Study. (2022).

Fam, A. (2022). Principles and performance analysis of regenerative braking systems in electric vehicles. *Journal of Electrical Engineering and Technology.*

Faghihian, H., et al. (2024). Battery management system integration for optimized energy recovery in EVs. *IEEE Transactions on Transportation Electrification.*

Faghihian, H., et al. (2024). Optimization of regenerative braking torque for enhanced energy recovery in urban driving cycles.

Farzana, S., & Bindu, P. (2022). Switched reluctance motors for robust EV regenerative braking applications.

Gilda, V., & Satarkar, R. (2020). Mean of Maximum defuzzification technique in fuzzy control systems. *International Journal of Fuzzy Systems.*

Gulhane, P., Patil, R., & Kulkarni, S. (2024). Fuzzy logic–based regenerative braking control for electric vehicles. *Journal of Electrical Engineering & Technology.*

Hamdan, A., et al. (2023). Efficiency improvement of regenerative braking systems using capacitor banks.

Harshavardhan, S., et al. (2024). Supercapacitor integration in parallel regenerative braking systems. *IEEE Access, 12,* 87654–87666.

Huja, A., & Jitham, P. (2014). Hybrid PID-ANFIS control strategies for electric vehicle regenerative braking. *Journal of Intelligent Transportation Systems.*

Irshana, R., & Vijayasree, P. (2025). Multiport bidirectional DC-DC converters for integrated energy management in EVs. *Energy Conversion and Management, 295,* 116974.

Jing-ming, W., et al. (2008). Simulation studies on energy recovery in parallel regenerative braking systems. *SAE Technical Paper 2008-01-1345.*

Kale, S., et al. (2023). Power electronic interfaces and energy reuse in electric vehicle regenerative braking. *IEEE Access.*

Kannan, R., et al. (2023). Bidirectional DC-DC converters for regenerative braking in electric vehicles. *IEEE Transactions on Power Electronics.*

Karabacak, M., & Uysal, S. (2020). Implementation of fuzzy logic controllers in blended regenerative and friction braking systems. *IEEE Transactions on Vehicular Technology.*

Kelin, R. (2015). PID control applications in regenerative braking systems. *Journal of Automotive Control Systems.*

Kumar, A. (2017). Defuzzification methods for fuzzy logic control in automotive applications. *Journal of Control Science and Engineering.*

Kumar, S., et al. (2021). Modified non-isolated bidirectional DC-DC converters for EV regenerative braking systems. *International Journal of Automotive Technology.*

Li, Y., Chen, S., & Xu, H. (2020). Optimized regenerative braking control for urban electric vehicles. *Energy Reports, 6*, 1123–1135.

Li, Y., Zhang, H., & Wang, J. (2023). Fuzzy logic and neural network control for EV regenerative braking systems. *International Journal of Automotive Technology.*

Liu, X. (2021). Intelligent control strategies for series regenerative braking in electric vehicles. *Journal of Automotive Engineering.*

Low, R., et al. (2022). Weight gain of battery and hydrogen zero-emission vehicles.

Mallick, S., & Das, A. (2021). Advances in defuzzification methods for adaptive fuzzy control. *Fuzzy Sets and Systems.*

Melis, E., & Chishty, F. (2013). Vehicle dynamics and energy recovery in regenerative braking. *SAE Technical Paper 2013-01-1234.*

Minarcin, J., et al. (2010). Dynamic torque calculation methods for regenerative braking systems. *SAE Technical Paper 2010-01-1234.*

Mohammad, A., & Jaber, R. (2022). Efficiency assessment of BLDC motors in electric vehicles.

Mondal, S., & Nandi, S. (2022). Improved parallel regenerative braking system for energy efficiency in electric vehicles. *Journal of Energy Storage, 50*, 104513.

Na, S., & Jing, L. (2012). Semi-linear defuzzification for improved fuzzy controller performance. *Journal of Intelligent Systems.*

Naseri, A., et al. (2017). Hybrid battery–supercapacitor energy storage in regenerative braking applications. *Journal of Power Sources, 348*, 68–78.

Patle, B., & Subha, K. (2023). Enhancing braking responsiveness in EVs using supercapacitors.

Qian, L., et al. (2018). Impact of regenerative braking on vehicle handling and braking performance.

Qian, L., Zhang, Y., & Wang, J. (2018). Cooperative control of regenerative and friction braking for electric vehicles.

Raimi, M., & Bakar, A. (2024). Sustainability assessment of battery technologies for EV regenerative braking.

Riyadi, M., & Setianto, D. (2019). Control strategies for BLDC motor–based regenerative braking systems.

Salari, P., et al. (2023). Control algorithm enhancements for improved energy efficiency in EV regenerative braking. *IEEE Transactions on Transportation Electrification.*

Samanci, E. (2023). Cost analysis of lead-acid vs lithium-based batteries for EV applications.

Savchenok, I. (2022). Adaptive PID and ANFIS integration for optimized regenerative braking performance. *International Journal of Automotive Engineering.*

Shanmugapriya, S., Rajesh, S., & Karthikeyan, R. (2024). Energy management and regenerative braking control using battery–supercapacitor hybrid storage in electric vehicles. *International Journal of Energy Research.*

Sim, H., et al. (2019). High-intensity regenerative braking performance and comfort assessment in EVs. *Journal of Vehicle Dynamics.*

Suresh, P., et al. (2022). Single-input multiple-output DC-DC converters for electric vehicle subsystems. *Journal of Power Electronics, 22*(5), 1183–1196.

Totev, S., Todorov, D., & Kitanov, V. (2019). Regenerative braking system for electric vehicles. *Proceedings of IEEE ELMA.*

Tousi, K., et al. (2016). Torque distribution strategies for combined regenerative and hydraulic braking. *IEEE Transactions on Vehicular Technology.*

Vasiljević, D., et al. (2022). Electromagnetic energy conversion in electric vehicle regenerative braking systems. *Energies.*

Wang, H., Liu, X., & Chen, Y. (2024). Safety-oriented regenerative braking control under emergency conditions.

Xu, L., Wang, Y., & Chen, Z. (2011). Anti-lock regenerative braking control for electric vehicles. *IEEE Transactions on Vehicular Technology.*

Xu, X., Lin, Y., & Li, Z. (2016). Knowledge-based regenerative braking control under varying road conditions.

Xue, L., et al. (2008). Comparison of electric motor types for EV conversions.

Xiao, L., et al. (2017). Safety analysis of series regenerative braking under varying load conditions. *Vehicle System Dynamics, 55*(9), 1321–1337.

Yildirim, S., et al. (2014). Switched reluctance motors in electric vehicle applications.

Yuantao, L., et al. (2019). Fuzzy logic–based torque allocation in parallel regenerative braking systems. *International Journal of Vehicle Design, 80*(4), 287–304.

Zhang, W., et al. (2008). Energy recovery performance of series regenerative braking systems in electric vehicles. *SAE Technical Paper 2008-01-1234.*

Zheng, L. (2022). Performance evaluation of permanent magnet synchronous motors for EVs.

Zhijian, L. (2006). Adaptive defuzzification techniques for fuzzy inference systems. *IEEE Transactions on Fuzzy Systems.*